Microglia overexpressing brain-derived neurotrophic factor promote vascular repair and functional recovery in mice after spinal cord injury

Fanzhuo Zeng[1, 2, 3], Yuxin Li[4], Xiaoyu Li[4], Xinyang Gu[4], Yue Cao[4], Shuai Cheng[1], He Tian[5, *], Rongcheng Mei[2, *], Xifan Mei[1, *]

https://doi.org/10.4103/NRR.NRR-D-24-00381

Date of submission: April 7, 2024

Date of decision: June 26, 2024

Date of acceptance: September 23, 2024

Date of web publication: October 22, 2024

From the Contents

Graphical Abstract

Microglia promote vascular repair and functional recovery after spinal cord injury through overexpressing BDNF

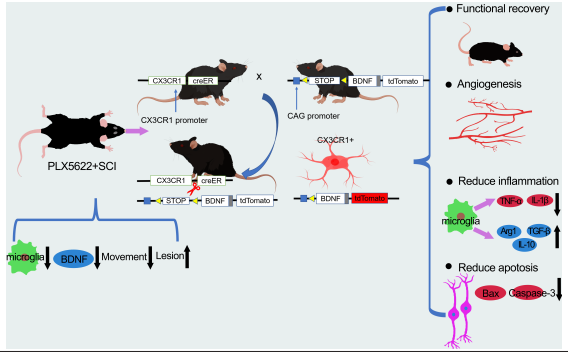

Abstract

Spinal cord injury represents a severe form of central nervous system trauma for which effective treatments remain limited. Microglia is the resident immune cells of the central nervous system, play a critical role in spinal cord injury. Previous studies have shown that microglia can promote neuronal survival by phagocytosing dead cells and debris and by releasing neuroprotective and anti-inflammatory factors. However, excessive activation of microglia can lead to persistent inflammation and contribute to the formation of glial scars, which hinder axonal regeneration. Despite this, the precise role and mechanisms of microglia during the acute phase of spinal cord injury remain controversial and poorly understood. To elucidate the role of microglia in spinal cord injury, we employed the colony-stimulating factor 1 receptor inhibitor PLX5622 to deplete microglia. We observed that sustained depletion of microglia resulted in an expansion of the lesion area, downregulation of brain-derived neurotrophic factor, and impaired functional recovery after spinal cord injury. Next, we generated a transgenic mouse line with conditional overexpression of brain-derived neurotrophic factor specifically in microglia. We found that brain-derived neurotrophic factor overexpression in microglia increased angiogenesis and blood flow following spinal cord injury and facilitated the recovery of hindlimb motor function. Additionally, brain-derived neurotrophic factor overexpression in microglia reduced inflammation and neuronal apoptosis during the acute phase of spinal cord injury. Furthermore, through using specific transgenic mouse lines, TMEM119, and the colony-stimulating factor 1 receptor inhibitor PLX73086, we demonstrated that the neuroprotective effects were predominantly due to brain-derived neurotrophic factor overexpression in microglia rather than macrophages. In conclusion, our findings suggest the critical role of microglia in the formation of protective glial scars. Depleting microglia is detrimental to recovery of spinal cord injury, whereas targeting brain-derived neurotrophic factor overexpression in microglia represents a promising and novel therapeutic strategy to enhance motor function recovery in patients with spinal cord injury.

Key Words: angiogenesis; apoptosis; brain-derived neurotrophic factor; colony stimulating factor 1 receptor; inflammation; microglia; motor function; spinal cord injury; vascular endothelial growth factor

Introduction

Spinal cord injury (SCI) poses a high risk of causing severe neurological dysfunction below the injured segment (Anderson et al., 2022). SCI is characterized by high disability and poor recovery, with current treatments remaining limited, resulting in a yearly increase in the number of patients suffering from motor function loss (Lee et al., 2014; Fan et al., 2024). In the early stages of SCI, inflammatory cytokine storms tend to worsen spinal cord lesions, with central microglia and peripheral mononuclear macrophages playing key roles (Brockie et al., 2024; Wang et al., 2024). Microglia, as the resident macrophages of the central nervous system (CNS), account for 5%–10% of CNS cells (Ginhoux et al., 2010; Kierdorf et al., 2013; Li et al., 2024; Tan et al., 2024; Zhou et al., 2024) and are involved in CNS development, homeostasis, and disease (Pang et al., 2022). They have been shown to be crucial for recovery from SCI (Sierra et al., 2010; Colonna and Butovsky, 2017). It has been demonstrated that microglia in neonatal mice promote scarless repair after SCI (Li et al., 2020). Microglia are involved in phagocytosis and clearance of cellular debris after SCI and mediate the production of healing scars after injury (Hakim et al., 2021; Brennan et al., 2022). Overactivated microglia exacerbate neuroinflammation and lead to increased cell death. The conventional view is that there are two main

[1]Department of Orthopedics, The Third Affiliated Hospital of Jinzhou Medical University, Jinzhou, Liaoning Province, China; [2]Department of Orthopedics, Xiangyang Central Hospital, Affiliated Hospital of Hubei University of Arts and Science, Xiangyang, Hubei Province, China; [3]Department of Neurobiology, School of Basic Medical Sciences, Guangdong-Hong Kong-Macao Greater Bay Area Center for Brain Science and Brain-Inspired Intelligence, Southern Medical University, Guangzhou, Guangdong Province, China; [4]Institute for Translational Brain Research, State Key Laboratory of Medical Neurobiology, MOE Frontiers Center for Brain Science, Fudan University, Shanghai, China; [5]Liaoning Provincial Collaborative Innovation Center for Medical Testing and Drug Research, Jinzhou Medical University, Jinzhou, Liaoning Province, China

***Correspondence to:** He Tian, PhD, tianhe@jzmu.edu.cn; Rongcheng Mei, PhD, meirch@163.com; Xifan Mei, PhD, meixifan@jzmu.edu.cn.
https://orcid.org/0000-0002-4452-8005 (Xifan Mei)

Funding: *This work was supported by the National Natural Science Foundation of China, Nos. 82072165 and 82272256 (both to XM); and the Key Project of Xiangyang Central Hospital, No. 2023YZ03 (to RM).*

How to cite this article: *Zeng F, Li Y, Li X, Gu X, Cao Y, Cheng S, Tian H, Mei R, Mei X (2026) Microglia overexpressing brain-derived neurotrophic factor promote vascular repair and functional recovery in mice after spinal cord injury. Neural Regen Res 21(1):365-376.*

phenotypes of activated microglia after SCI, termed M1 and M2 (Tang and Le, 2016; Butovsky and Weiner, 2018). After SCI, microglia change from a ramified shape to an amoeboid shape. Activation of microglia is initiated by the removal of inhibitory neural signals, as well as by the activation of corresponding receptors by damage-associated molecular patterns (Castro-Gomez and Heneka, 2024; Liu et al., 2024). Among them, classically activated (M1) microglia, which mainly have pro-inflammatory effects, promote the synthesis of inflammatory mediators such as tumor necrosis factor-α (TNF-α), interleukin (IL)-1β, IL-6, glutamate, inducible nitric oxide synthase, peroxides, reactive oxygen species (ROS), matrix metalloproteinases (MMPs), and chemokines (CCL2, CXCL9), cause apoptosis and secondary damage, and have obvious neurotoxic effects that aggravate tissue damage and neuronal apoptosis (Colonna and Butovsky, 2017; Wang et al., 2023a; Zeng et al., 2024). Alternatively activated (M2) microglia mainly release anti-inflammatory factors such as Arg1, CD206, IL-4, and IL-10, as well as a variety of neurotrophic factors, such as brain-derived neurotrophic factor (BDNF), glial cell–derived neurotrophic factor, insulin-like growth factor 1, and transforming growth factor β (Prinz et al., 2019; Borst et al., 2021). They play an important role in angiogenesis, promotion of myelin sheath regeneration, axon growth, tissue repair, and regulation of inflammation. Regulating changes in microglial phenotypes after SCI is promising for the treatment of SCI, but the roles of the different phenotypes in different stages of SCI and the underlying mechanisms remain to be clarified. Furthermore, single-cell sequencing and other technologies have shown that microglia undergo more complex transcriptomic changes at different stages of SCI than previously thought, resulting in more phenotypes than just M1 and M2 (Li et al., 2022a; Matson et al., 2022).

BDNF is the most abundant neurotrophic factor in the CNS. It was first extracted and purified from porcine brain by Professor Barde, and was shown to support the survival of sensory neurons and the growth of nerve fibers in chick embryos (Barde et al., 1982). BDNF is a small dimeric protein. The monomer is secreted as a mature polypeptide consisting of 119 amino acid residues. The relative molecular mass of the monomer is 13.5 kDa, while the relative molecular mass of the mature dimeric form is about 28 kDa. The relative molecular mass of the immature form is about 35 kDa or 45 kDa (Mowla et al., 2001; Egan et al., 2003). There are two main BDNF receptors: the high-affinity tyrosine kinase receptor TrkB, a transmembrane protein located on the nerve cell membrane, and the low-affinity neurotrophic factor receptor p75 ($p75^{NTR}$) (Chao and Hempstead, 1995; Meeker and Williams, 2014; Bathina and Das, 2015). The precursor form of BDNF, pro-BDNF, has high affinity for $p75^{NTR}$, which, when activated, promotes apoptosis and inflammatory signaling in neurons and glial cells by inducing JNK and NF-kB expression (Lima Giacobbo et al., 2019). The mature form of BDNF has high affinity for TrkB, which plays an important role in maintenance of nerve growth, neuronal differentiation, and neuronal survival. BDNF can promote recovery from SCI through a variety of neural mechanisms, such as promoting neuronal cell survival by inducing the production of anti-apoptotic factors, inhibiting oxidative stress by up-regulating superoxide dismutase production, and promoting neurogenesis and axon outgrowth (Cheng et al., 2017; Sasi et al., 2017). In addition, after SCI, the blood–spinal cord barrier is disrupted, and the neurovascular unit is damaged due to mechanical injury. One *in vitro* study demonstrated that BDNF promotes the production of vascular endothelial growth factor (VEGF) (Mori et al., 2018), which may facilitate reconstruction of the neurovascular unit after SCI and promote blood vessel and nerve neogenesis and growth after SCI. While BDNF in the CNS is primarily derived from neurons and astrocytes (Lessmann and Brigadski, 2009; Zhang et al., 2014), recent studies have shown that microglia-derived BDNF is important for neuronal and synapse formation, learning, and promoting neural precursor cell proliferation and neurogenesis (Parkhurst et al., 2013; Zhang et al., 2021). Little is known about the differences among BDNF derived from microglia and that derived from other cellular sources, but some studies have shown that microglia-derived BDNF is very important for normal mouse function (Parkhurst et al., 2013; Zhang et al., 2021; Wang et al., 2023b). Thus, what the specific features of microglia-derived BDNF are that exert this effect is an interesting and important question that should be explored in further in-depth studies. Microglia and astrocytes are the main sources of BDNF after SCI (Tsuda et al., 2005; Chiang et al., 2012; Smith, 2014), but BDNF expression is only high in the acute phase after SCI and does not remain elevated. More BDNF is produced at 24 hours and 5 days after SCI, but BDNF expression levels return to normal on day 14 after SCI. In addition, spinal cord dorsal horn neurons, as well as peripheral T cells, produce BDNF (Zhou et al., 2021; Tang et al., 2022).

Colony stimulating factor 1 receptor (CSF1R) is a crucial receptor expressed on the surface of microglia that is essential for their survival (Elmore et al., 2014). Therefore, the role of microglial deficiency in CNS disorders can be effectively assessed using the CSF1R inhibitor PLX5622. Recent studies have indicated that removing microglia facilitates recovery from traumatic brain injury and SCI, as well as Alzheimer disease (Willis et al., 2020; Wang et al., 2023b), However, most of the models used in these studies were based on repopulation after microglia depletion. Continuous removal of microglia has been found to be detrimental to SCI, affecting astrocyte growth after injury (Bellver-Landete et al., 2019).

Effective therapeutic measures for SCI are lacking, which is an important medical concern worldwide. Microglia play a very important role in SCI, but the relevant mechanism is still unclear. In this study, we used a microglia depletion model and constructed transgenic mice in which BDNF is specifically overexpressed by microglia. The role of microglia-derived BDNF in motor function recovery and angiogenesis after SCI was investigated, and the results provide new avenues for the treatment of SCI.

Methods

Animals

Adult C57 BL/6J (wild-type [WT]) mice, male and female, weighing 20–28 g and aged 8–10 weeks, were obtained from Charles River (Zhejiang, China, license No. SCXK (Zhe) 2019-0001). The LSL-$BDNF^{+/+}$-tdTomato mice were generously provided by Fudan University (generated by Biocytogen, Beijing, China, Item No. EGE-LYX-032-A). Using mice prepared with the EGE system developed by Biocytogen based on CRISPR/Cas9, CAG-loxP-STOP-loxP-BDNF-IRES-tdTomato-WPRE-pA was inserted at the ROSA26 site. Polymerase chain reaction (PCR) and Southern blot were used to screen for mice with the correct gene recombination, and positive F1 mice were verified using a 5′ probe-2 and a WPRE probe at the same time. The promoter is CAG, and the cis-acting element is WPRE. The CX3CR1 $creER^{+/+}$ mice (male and female, weighing 20–28 g and aged 8 weeks) were purchased from Jackson Lab (Bar Harbor, ME, USA, Cat# 020940, RRID: IMSR_JAX:020940), The TMEM119 $creER^{+/+}$ mice (male and female, weighing 20–28 g and aged 8 weeks) were purchased from Jackson Lab (Cat# 031820, RRID: IMSR_JAX:031820). The CX3:BDNF mice were generated by crossing CX3CR1 $creER^{+/+}$ and LSL-$BDNF^{+/+}$-tdTomato mice, while the TMEM:BDNF mice were produced by crossing TMEM119 $creER^{+/+}$ and LSL-$BDNF^{+/+}$-tdTomato mice. Animals were randomly assigned to groups according to the genotype required for the experiment (**Additional Figure 1**). For part 1, WT mice were randomized to sham, SCI, and SCI + PLX5622 groups. For part 2, WT mice were randomized to sham, SCI, and SCI-CX3:BDNF groups. For part 3, WT mice were randomized to sham, SCI, SCI-TMEM:BDNF, SCI-CX3:BDNF + PLX73086 groups. In addition, we examined the clearance efficiency of PLX5622 and PLX73086 using WT mice, and the labeling efficiency of transgenic mice was tested using CX3:BDNF mice and TMEM:BDNF mice. Mice that died during the experimental period were replaced with other mice of the same genotype treated under the same experimental conditions and housed in the same environment. All animal experiments were approved by the Ethical Committee of Care and Use of Laboratory Animals at Jinzhou Medical University (approval No. 2022017) and reported according to the Animal Research: Reporting of *In Vivo* Experiments (ARRIVE) guidelines (Percie du Sert et al., 2020).The mice were reared in the Experimental Animal Center of Jinzhou Medical University in a specific pathogen–free environment at 22 ± 2°C with a 12/12-hour light/dark cycle and six mice per cage.

Spinal cord crush injury model

A mouse spinal cord T10 segment crush injury model was established following a previously published procedure (Li et al., 2020). The mice were anesthetized using isoflurane (RWD, Shenzhen, China, Cat# R510-22) and an anesthesia machine (induction concentration 3%, maintenance concentration 1%, flow rate 0.6–1 L/min). Dorsal hair was removed, the area was disinfected with iodophor, and a 1.5-cm incision was made at the T10 segment of the spinal cord to locate the T10 vertebral body on the tenth rib. A T10 laminectomy was then performed to expose the spinal cord. In brief, a midline incision was made over the thoracic vertebrae, followed by a T9–T11 laminectomy. Tips of 0.1-mm forceps were carefully inserted on either

side of the cord to encompass the full width of the cord and then gently scraped across the bone on the ventral side to not spare any tissue ventrally or laterally. The spinal cord was fully crushed for 2 seconds with the 0.1-mm forceps. The muscles were then sutured, and the skin was closed. The mice were then disinfected again with iodophor. Immediately after the crush injury, edema and ecchymosis appeared, resulting in a reduction in the motor behavior score to 0 on the basso mouse scale (BMS) after awakening from anesthesia (Basso et al., 2006; Xu et al., 2023). The mice lost motor function in the hindlimb developed urinary retention, and exhibited dragging of the hindlimb on the ground, with an inability to lift the tail. After surgery, each mouse was placed in a holding cage (on a heating pad in winter or cold days until awakening), with feed placed on the mat for easy access. Following injury, the bladders of the mice were manually emptied twice daily until they were euthanized.

Pharmacological microglia depletion

To deplete microglia in the spinal cords of WT mice, we used AIN76A feed (SYSE Bio, Changzhou, China, item No. PD1001) supplemented with PLX5622, a CSF1R inhibitor that can cross the blood–brain barrier (SYSE Bio, item No. D20010801, PLX5622 at 1200 mg/kg). To remove peripheral macrophages from CX3:BDNF mice, we used AIN76A feed supplemented with PLX73086, a CSF1R inhibitor that does not cross the blood–brain barrier (ResearchDiets, New Brunswick, NJ, USA. Item No. D15120708i, PLX73086 at 200 mg/kg). Control and untreated mice were fed the AIN76A control diet (SYSE Bio, item No. PD1001) with no supplements.

Basso mouse scale behavioral scores

The BMS score is frequently used to evaluate the motor function of mice (Basso et al., 2006). The behavioral scores of mice after SCI were analyzed by two investigators experienced in using the BMS scale on the day before and 1, 3, 7, 14, 21, and 28 days after SCI. A score of 0 indicated no ankle and paw movement, and a score of 9 indicated normal motor function. The average of the two scores was then used for analysis.

Rotarod test

On the 28th day after SCI, the rotarod experiment was performed. The speed of the spinning rod was accelerated from 5 r/min to 40 r/min over 5 minutes. The mice were allowed to adapt to the rod prior to the formal experiment, which was repeated five times. The amount of time that each mouse was able to stay on the spinning rod was recorded, along with the rotational speed when the mouse fell. A UGO basile RotaRod (UGO Basile, Vittorio, Italy, 47650) was used in these experiments, which were designed to test motor function and muscle coordination to analyze the effects of treatment after SCI.

Footprint analysis

A quiet, temperature-controlled room was used for the behavioral studies. Footprint analysis was performed based on a previously reported modified footprint analysis method (Kunkel-Bagden et al., 1993; Bradbury et al., 2002). A runway 100 cm long, 7 cm wide, and 7 cm high was constructed out of cardboard, and white paper was placed along the runway. Food, used bedding, and cotton were placed at the end of the runway to guide the mice from the beginning to the end of the runway. Each mouse was placed at the beginning of the runway and allowed to move independently on the runway; the mice were familiarized with the runway and the environment before the formal experiment was performed. For the formal experiment, on the 28th day after the SCI each mouse's front paws were dipped in black ink and their back paws in red ink, and they were allowed to traverse the runway three times (using a fresh paper liner each time). The step length (distance between the front and rear paws), step width (distance between the two paws), and number of steps taken with the rear paws were determined.

Genotyping

Transgenic mice (CX3CR1 creER, TMEM119 creER, CX3:BDNF, TMEM:BDNF) were divided into cages at 4 weeks of age and genetically characterized. A small piece of tissue was cut from the tail of the mice, and DNA was extracted from the tissue by incubating at 98°C for 1 hour with 100 µL of alkali (25 mM NaOH + 0.2 mM EDTA) and then neutralizing with 100 µL of tris hydrochloric acid. PCR (Vazyme, Nanjing, China; 2x rapid tap master mix, Cat# P222) and agarose gel electrophoresis were then performed, followed by imaging with a molecular imager (**Additional Figure 2**). Primer information for gene identification is shown in **Additional Table 1**.

Tamoxifen gavage

To induce recombination of the CX3CR1 creER$^{-/+}$:LSL-BDNF$^{-/+}$-tdTomato and TMEM119 creER$^{-/+}$:LSL-BDNF$^{-/+}$-tdTomato genes, mice were given tamoxifen (Aladdin, Shanghai, China, Cat# T137974-5g) by gavage for 5 consecutive days at 150 mg/kg per day (dissolved in 1:25 ethanol/olive oil). First, the tamoxifen solid was weighed using an electronic scale, then anhydrous ethanol was added, followed by olive oil. The tube containing the mixture was wrapped tin foil to protect it from light, and the mixture was then heated in a water bath for 1 hour at 42°C, followed by shaking at room temperature overnight. The dissolved tamoxifen was administered by gavage the next day using a 1-mL syringe.

RNA isolation and quantitative reverse transcription-polymerase chain reaction

The mice were anesthetized with isoflurane, euthanized, and placed in an icebox. After rapid PBS perfusion, the spinal cords of the adult mice were rapidly dissected out. The central 4 mm of the lower thoracic lesion, including the core of the lesion and 2 mm rostral and caudal, were then rapidly removed. The spinal cord was then placed in an enzyme-free centrifuge tube, and 1 mL of Trizol (Tsingke Biotech, Beijing, China, Cat# TSP401) was added. Magnetic beads were used to fully homogenize the tissue using a tissue grinder. RNA was extracted then with Trizol following the steps in the kit instructions. Once the total RNA was dried, 20 µL of enzyme-free water was added to dissolve the RNA. The concentration of the RNA and the A260/A280 and A260/A230 ratios were measured using a nanodrop spectrophotometer. The sample concentration was adjusted to 400 ng/µL with enzyme-free water, and a reverse transcription kit from Vazyme (Cat# R323-01) was used to perform reverse transcription. After the reaction was complete, 180 uL of enzyme-free water was added to dilute the cDNA, which was then stored at –80°C. Forward and reverse primers were synthesized and ordered from Shanghai Tsingke Biotechnology; the sequences are shown in **Additional Table 2**. A fluorescent quantitative PCR kit from Vazyme (Cat# Q711-02) was used to detect the expression levels of the target genes in the samples. The 20-µL quantitative PCR reaction mixture contained 2 µL cDNA template, 0.4 µL (10 µM) forward primer, 0.4 µL (10 µM) reverse primer, 10 µL qPCR Master Mix, and 7.2 µL ddH_2O. The fluorescent signals were captured using a fluorescence PCR instrument (ABI Stepone plus, Carlsbad, CA, USA). Relative expression levels were determined using the $2^{-\Delta\Delta CT}$ method and normalized to glyceraldehyde-3-phosphate dehydrogenase (GAPDH).

Blood flow measurements

Blood flow was measured in mice using a Laser speckle blood flow meter (Perimed, Stockholm, Sweden. Version: Pericam PSI HR) before SCI, 5 minutes after injury, and on the 28th day after injury was induced. The mice were anesthetized with isoflurane, and the injured site was exposed for blood flow measurement.

Tissue section preparation

The mice were euthanized by inhalation of an overdose of isoflurane. The spinal cords were then removed and placed in 4% PFA for fixation overnight. Next, the spinal cord was rinsed with PBS and dehydrated in PBS containing 30% sucrose for 4 days. The spinal cords were then embedded in OCT and frozen at –80°C. The frozen embedded tissues were then sliced at a thickness of 30 µm.

Immunofluorescence staining

The spinal cord tissues were sectioned and washed three times with PBS. The tissue slices were then blocked with 4% DPBST (PBS containing 4% normal donkey serum and 0.3% Triton X-100) at room temperature for 2 hours. After blocking for 2 hours, the 4% DPBST was removed, the corresponding primary antibody was added, and the slices were incubated at 4°C overnight. The tissues were removed the next day and rewarmed at room temperature for 1 hour. Then, the primary antibody was removed, and the tissue slices were washed with PBS three times for 5 minutes each. Next, secondary antibody containing 4′,6-diamidino-2-phenylindole (DAPI; 1:1000; Sigma-Aldrich, St. Louis, MO, USA. Cat# D9542-10MG), diluted in normal donkey serum (Jackson, Cat# 017-000-121), was added, and the slices were incubated at room temperature for 2 hours. After 2 hours, the tissue slices were washed with PBS three times for 5 minutes each, then allowed to dry. The slices were mounted on slides with anti-fluorescence quencher, and the coverslips were

sealed with clear nail polish. All primary and secondary antibodies were diluted in PBST containing 1% NDS and are listed in **Table 1**. Finally, the tissue sections were observed using a fluorescence microscope (Olympus VS200, Tokyo, Japan; Nikon C2 Confocal microscope, Tokyo, Japan). Labeled cells were counted using ImageJ (version 1.6.0; National Institutes of Health, Bethesda, MD, USA) software (Schneider et al., 2012). For specific cell counts, the data are expressed as the number of cells/section. For double staining, data are expressed as the ratio of double-positive to single-positive cells. ImageJ software was used to measure mean fluorescence intensity in target cells.

Terminal deoxynucleotidyl transferase dUTP nick end labeling assay

A terminal deoxynucleotidyl transferase dUTP nick end labeling (TUNEL) assay was performed at 24 hours after SCI (TUNEL kit, Elabscience, Wuhan, China. Cat# E-CK-A321). We primarily examined the proportion of apoptotic cells and the number of neurons 24 hours after SCI, because according to previous studies, TUNEL-positive neuroglial cells are present at all stages of SCI from 4 hours to 14 days after SCI but are most numerous in the lesion area 24 hours after SCI. In addition, TUNEL-positive neurons are mainly confined to the general lesion area 4–24 hours after injury, although within 7 days of SCI, the lesion area enlarges and cavitates, resulting in a second wave of TUNEL-positive glial cells in the white matter surrounding the lesion and extending at least a few millimeters away from the center of the lesion (Liu et al., 1997; Fang et al., 2021; Xu et al., 2023). The mouse spinal cords were perfused with PFA and dehydrated, then frozen and sectioned at a thickness of 30 μm. The apoptotic signals were subsequently detected following the steps outlined in the kit instructions. The samples were sealed with an anti-fluorescence quenching sealing agent (Fluromount, SouthernBiotech, Birmingham, Alabama, USA, Cat# 0100-01). Finally, the sections were observed using a fluorescence microscope (Olympus VS200, Tokyo, Japan; Nikon C2 Confocal microscope, Tokyo, Japan). Labeled cells were counted using ImageJ software.

Statistical analysis

At least six biological replicates were performed for all animal experiments, and at least three technical replicates were included for all samples. GraphPad Prism (San Diego, CA, USA, www.graphpad.com. Version: 9.5.0) was used for general data visualization and statistical analyses. Unpaired *t*-test was used for comparisons between two groups, while one-way analysis of variance with Bonferroni *post hoc* test or two-way analysis of variance with Bonferroni *post hoc* test was used for comparisons among multiple groups. BMS was analyzed using two-way repeated-measures analysis of variance with Bonferroni *post hoc* test. Data in all figures are shown as the mean ± SD. A *P*-value < 0.05 was considered statistically significant.

Results

Continuous removal of microglia aggravates spinal cord injury

To investigate the effects and mechanisms of microglia depletion on SCI, we subjected mice to spinal cord crush injury (**Figure 1A**) and provided them with a PLX5622-containing diet starting 14 days before injury and continuing until the 28th day after injury (**Figure 1B**). To assess the depletion efficiency of PLX5622, we administered the PLX5622-containing diet to WT uninjured mice for 14 days and observed a marked reduction in the number of microglia in the spinal cord after 2 weeks of consuming the PLX5622-containing diet compared with the normal diet group (**Figure 1C** and **Additional Figure 3A**).

For all subsequent experiments, we used the established mouse model of SCI in which microglia had been cleared via PLX5622 administration. We evaluated hindlimb motor function on day 1 before SCI, as well as on days 1, 3, 7, 14, 21, and 28 after injury, using the BMS scale. Our findings revealed that continuous removal of microglia was detrimental to the recovery of hindlimb motor function after SCI (**Figure 1D**). Previous studies have indicated that, in response to SCI, microglia are heavily activated and secrete large amounts of inflammatory factors that hinder recovery (Liu et al., 2020; Li et al., 2022b; Gong et al., 2023). Although microglia removal reduced the number of activated CD68^{+} microglia on day 14 after SCI (**Figure 1E–G**), unexpectedly, the average lesion size in the microglia removal (SCI + PLX5622) group was larger than that in the control group on day 14 after SCI. Additionally, the removal of microglia affected astrocyte proliferation (**Figure 1H** and **Additional Figure 4**), the formation of glial cell scars was reduced, lesion area increased, and infiltration of F4/80-positive peripheral macrophages increased (**Figure 1H–J**). RT-qPCR analysis demonstrated downregulation of BDNF mRNA levels after SCI following the removal of microglia (**Figure 1K**). This finding was particularly unexpected because, in the CNS, the main sources of BDNF are neurons and astrocytes, suggesting that the removal of microglia may reduce the expression of microglia-derived BDNF after SCI or affect the secretion of BDNF from other cellular sources. This indicates that microglia play a crucial role in lesion improvement and motor function recovery after SCI by modulating astrocyte proliferation and BDNF secretion.

Table 1 | **Antibodies used for immunofluorescence staining**

Antibodies	Markers	Dilutions	Cat#	RRID	Suppliers
Primary antibodies					
Rabbit anti-Iba1	Microglia	1:500	019-19741	AB_839504	Wako, Osaka, Tokyo
Goat anti-Iba1	Microglia	1:500	ab5076	AB_2224402	Abcam, Cambridge, UK
Rabbit anti-fibronectin	fibronectin	1:500	AB2033	AB_2105702	Millipore, Bedford, MA, USA
Rat anti-CD68	actived microglia and macrophage	1:500	MCA1957	AB_322219	Bio-Rad, Hercules, CA, USA
Rabbit anti-GFAP	astrocyte	1:500	ab7260	AB_305808	Abcam
Rabbit anti-Arg1	M2 type microglia	1:500	ab91279	AB_10674215	Abcam
Rat anti-F4/80	macrophage	1:200	123101	AB_893504	BioLegend, SanDiego, CA, USA
Rabbit anti-P2RY12	resting state microglia	1:500	HPA014518	AB_2669027	Sigma-Aldrich, St. Louis, MO, USA
Chicken anti-mCherry	tdTomato proteins (a red fluorescent protein)	1:500	ab205402	AB_2722769	Abcam
Rabbit anti-BDNF	BDNF	1:500	ab108319	AB_10862052	Abcam
Goat anti-5-HT	serotonin positive axons	1:5000	20079	AB_572262	Immunostar, Hudson, WI, USA
Rat anti-CD31	vessel	1:30	550274	AB_393571	BD bioscience, Franklin Lakes, NJ, USA
Rabbit anti-NeuN	Neuron	1:500	ab177487	AB_2532109	Abcam
Rabbit anti-IL-1β	IL-1β	1:500	12703S		Cell Signaling Technology, Danvers, MA, USA
Rabbit anti-MBP	myelin sheath	1:500	ab218011	AB_2895537	Abcam
Secondary antibodies					
AF488 donkey anti-rabbit		1:1000	711-545-152	AB_2313584	Jackson, West Grove, PA, USA
AF568 donkey anti-rat		1:1000	ab175475	AB_2636887	Abcam
AF568 donkey anti-goat		1:1000	A11057	AB_2534104	Invitrogen, Carlsbad, CA, USA
Cy3 donkey anti-chicken		1:1000	703-165-155	AB_2340363	Jackson
AF568 donkey anti-rabbit		1:1000	A10042	AB_2534017	Invitrogen
AF647 donkey anti-rat		1:1000	A48272	AB_2893138	Invitrogen
AF647 donkey anti-goat		1:1000	705-605-003	AB_2340436	Jackson
AF647 donkey anti-chicken		1:1000	703-605-155	AB_2340379	Jackson

5-HT: 5-Hydroxytryptamine; BDNF: brain-derived neurotrophic factor; GFAP: glial fibrillary acidic protein; Iba1: ionized calcium binding adaptor molecule 1; IL: interleukin; MBP: myelin basic protein.

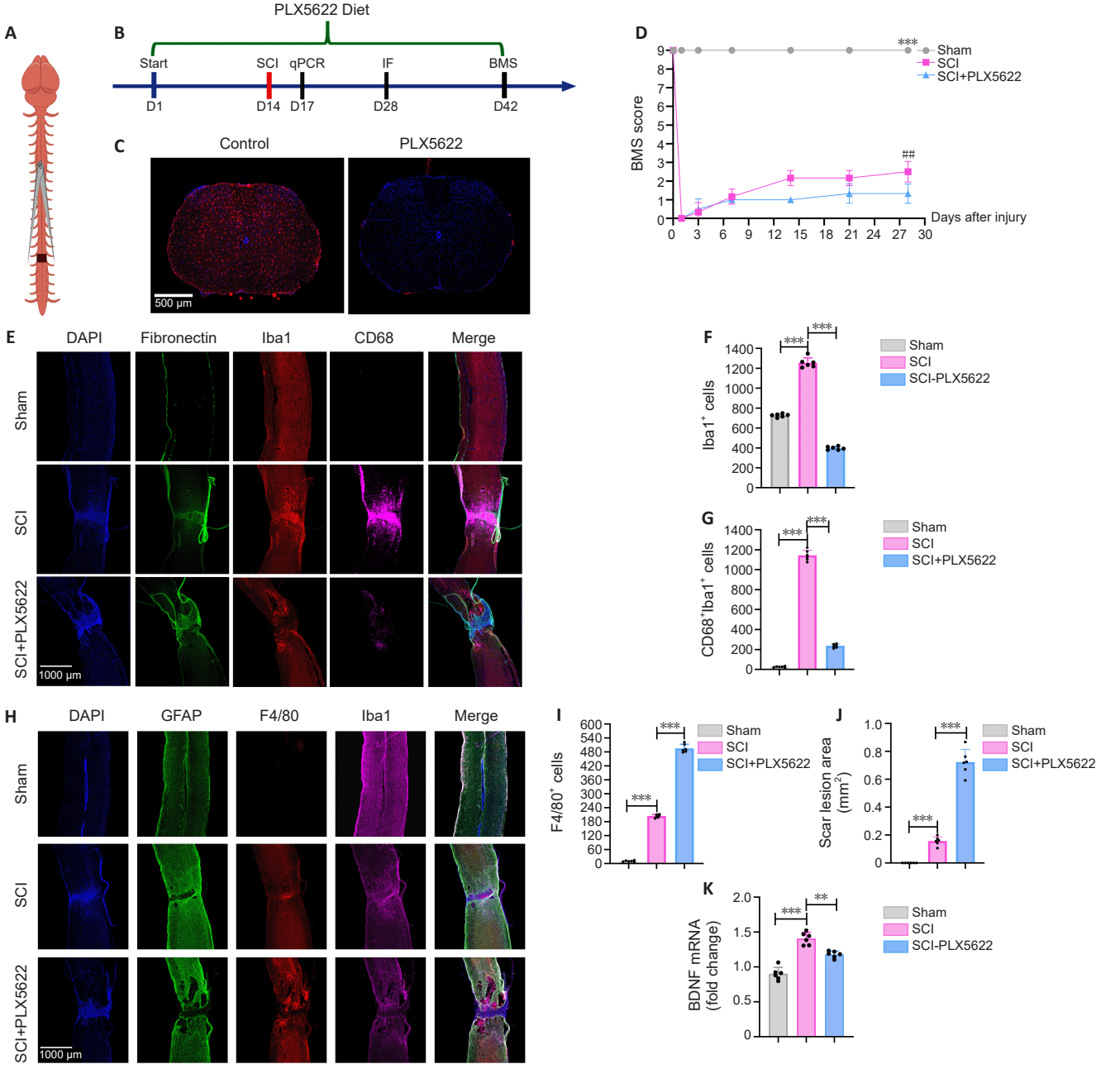

Figure 1 | **Microglia are essential for recovery from spinal cord injury, and their removal is detrimental to recovery from spinal cord injury.**

(A) Spinal cord crush injury at the T10 segment. (B) Experimental timeline of sustained microglia clearance and spinal cord injury. (C) Immunofluorescence demonstrated the efficient depletion of microglia (red) in wild-type mice. Scale bar: 500 μm. Nuclei: blue, microglia: red. (D) Microglia depletion is not conducive to recovery from spinal cord injury, based on BMS scores (***P < 0.001, sham group *vs*. SCI group; ##P < 0.01, SCI group *vs*. SCI + PLX5622 group). (E–G) A CSF1R inhibitor reduces the number of microglia (Iba1$^+$ cells) and CD68-positive cells after spinal cord injury on day 14. Scale bar: 1000 μm. Nuclei: blue, fibronectin: green, Iba1: red, CD68: magenta. (H–J) Microglia depletion results in a larger lesion at day 14 after spinal cord injury and increases infiltration of F4/80-positive peripheral macrophages. Scale bar: 1000 μm. Nuclei: blue, glial fibrillary acidic protein (GFAP, marker of astrocyte): green, F4/80: red, Iba1: magenta. (K) Microglia depletion reduces BDNF production on day 3 after spinal cord injury. Two-way repeated-measures analysis of variance with Bonferroni *post hoc* test (D); one-way analysis of variance with Bonferroni *post hoc* test (F, G, I, J, K). **P < 0.01, ***P < 0.001. All mice were C57BL/6J (wild-type) mice, and there were six mice per group. BDNF: Brain-derived neurotrophic factor; BMS: basso mouse scale; D1: day 1; Iba1: ionized calcium binding adaptor molecule 1; PLX5622: colony stimulating factor 1 receptor (CSF1R) inhibitor; SCI: spinal cord injury.

Construction of mice whose microglia conditionally overexpress brain-derived neurotrophic factor

Previous studies have demonstrated the crucial role of microglia-derived BDNF in the regulation of neurogenesis and neuronal synaptic plasticity (Parkhurst et al., 2013; Zhang et al., 2021; Wang et al., 2023b). Our results also indicate that the removal of microglia is detrimental to recovery from SCI and affects BDNF production after SCI, suggesting the potentially crucial role of microglia-derived BDNF. Therefore, we generated mice whose microglia conditionally overexpress BDNF (**Figure 2A** and **B**). The labelling rate of tdTomato positive microglia in CX3:BDNF mice reached nearly 98% after tamoxifen administration via gavage (**Figure 2C** and **D**). Initially, we examined *BDNF* expression after activation in CX3:BDNF mice and found that the *BDNF* mRNA content in the spinal cord of mice on day 14 after completion of tamoxifen gavage was higher than that in mice that received tamoxifen gavage after 7 days and also higher than that in the WT group (Activation here refers to the conditional overexpression of the BDNF gene in microglia of CX3:BDNF mice achieved by administering tamoxifen. The metabolites of tamoxifen bind to estrogen receptors (ER), leading to the release of Cre into the nucleus and subsequent recombination at LoxP sites) (P < 0.001; **Figure 2H** and **I**). Subsequently, we assessed BDNF mRNA expression in the spinal cord of mice on the third day after SCI and observed that the CX3:BDNF group exhibited higher levels compared with the WT group and the WT-SCI group (P < 0.001; **Figure 2G**). Furthermore, we detected BDNF expression in the spinal cord adjacent to the injury site through immunofluorescence on the 28th day after SCI and found that the CX3:BDNF group maintained stable overexpression of BDNF on the 28th day after SCI (P < 0.001; **Figure 2E**

and **F**). However, we found that, although BDNF protein and mRNA levels in CX3:BDNF in transgenic mice were markedly increased, colocalization of BDNF and ionized calcium binding adaptor molecule 1 (Iba1) was relatively low. This is most likely due to the fact that BDNF is a secreted protein, and thus BDNF overexpressed by microglia is secreted outside of the cells. Moreover, we found that colocalization of BDNF and Iba1 was markedly increased in the CX3:BDNF group compared with WT group, and there was almost no colocalization of BDNF and Iba1 in the WT group.

Brain-derived neurotrophic factor overexpression by microglia facilitates the recovery of hindlimb motor function after spinal cord injury

To investigate the impact of BDNF overexpression by microglia following SCI, we administered tamoxifen to CX3:BDNF mice via gavage for 5 consecutive days and induced SCI after 14 days. The spinal cord tissues were then collected on the third day post-injury and used for qPCR and immunofluorescence assays. BMS scoring was conducted 1, 3, 7, 14, 21, and 28 days after SCI, and rotarod and gait analysis experiments were performed on the 28th day post-injury (**Figure 3A**). Our findings revealed an improvement in hindlimb motor function and coordination following SCI, with the SCI-CX3:BDNF group exhibiting greater step width, step length, and number of footprints compared with the SCI-WT group ($P < 0.001$; **Figure 3B–E**). Additionally, in the open field experiment, mice in the SCI-CX3:BDNF group displayed more frequent standing, paw touching on the ground, and tail raising compared with the SCI-WT group ($P < 0.001$; **Figure 3F**). Furthermore, the BMS scores of the SCI-CX3:BDNF mice were higher than those of the SCI-WT mice ($P < 0.001$; **Figure 3G**). In the rotarod experiment, mice in the SCI-CX3:BDNF group demonstrated better performance and tolerated higher rotational speeds compared with the SCI-WT group ($P < 0.001$), as indicated by the fall latency from the rotarod (**Figure 3H–J**). These results suggest that BDNF overexpression in mouse microglia facilitates recovery of hindlimb motor function in mice with SCI.

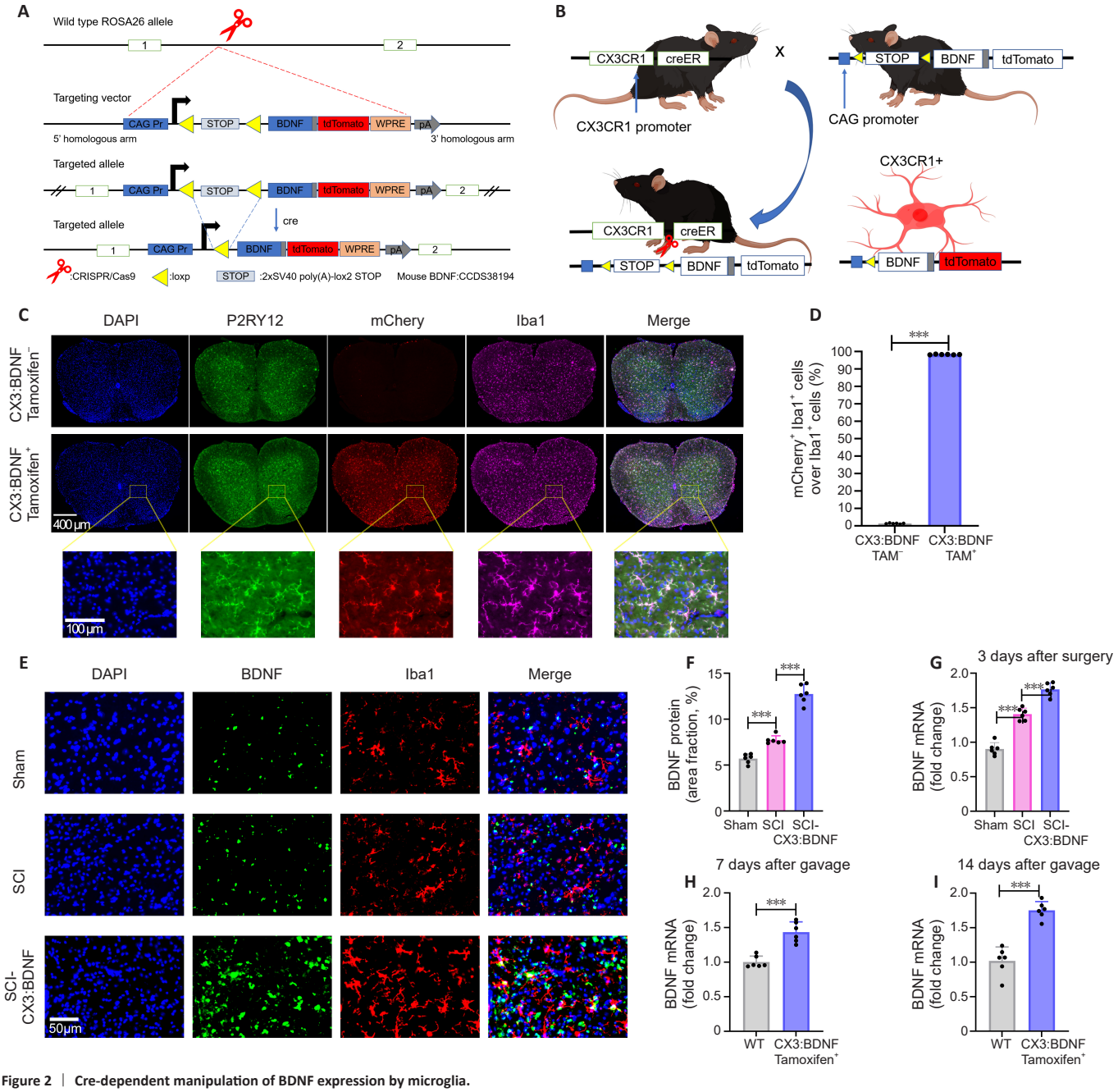

Figure 2 | **Cre-dependent manipulation of BDNF expression by microglia.**

(A, B) Construction of transgenic mice. (C, D) Assessment of induction efficiency in the CX3:BDNF mice. Scale bar: 400 μm. Scale bar in enlarged figures: 100 μm. Nuclei: blue, P2RY12: green, mCherry (mCherry is used to label tdTomato proteins, a red fluorescent protein. mCherry labelled cells here are mainly CX3CR1 positive cells): red, Iba1: magenta. (E–I) Evaluation of BDNF expression in microglia in transgenic mice before and after spinal cord injury. Scale bar: 50 μm. Nuclei: blue, BDNF: green, Iba1: red. Unpaired *t*-test (D, H, I); One-way analysis of variance with Bonferroni *post hoc* test (F, G). ***$P < 0.001$. The mice used in Figure C and D were CX3:BDNF, and there were six mice in each group. In E–I, C57BL/6J (wild-type) mice were used in the sham, SCI, and WT groups, and CX3:BDNF mice were used in the SCI-CX3:BDNF group, and there were six mice in each group. BDNF: Brain-derived neurotrophic factor; Iba1: ionized calcium binding adaptor molecule 1; WT: wild-type.

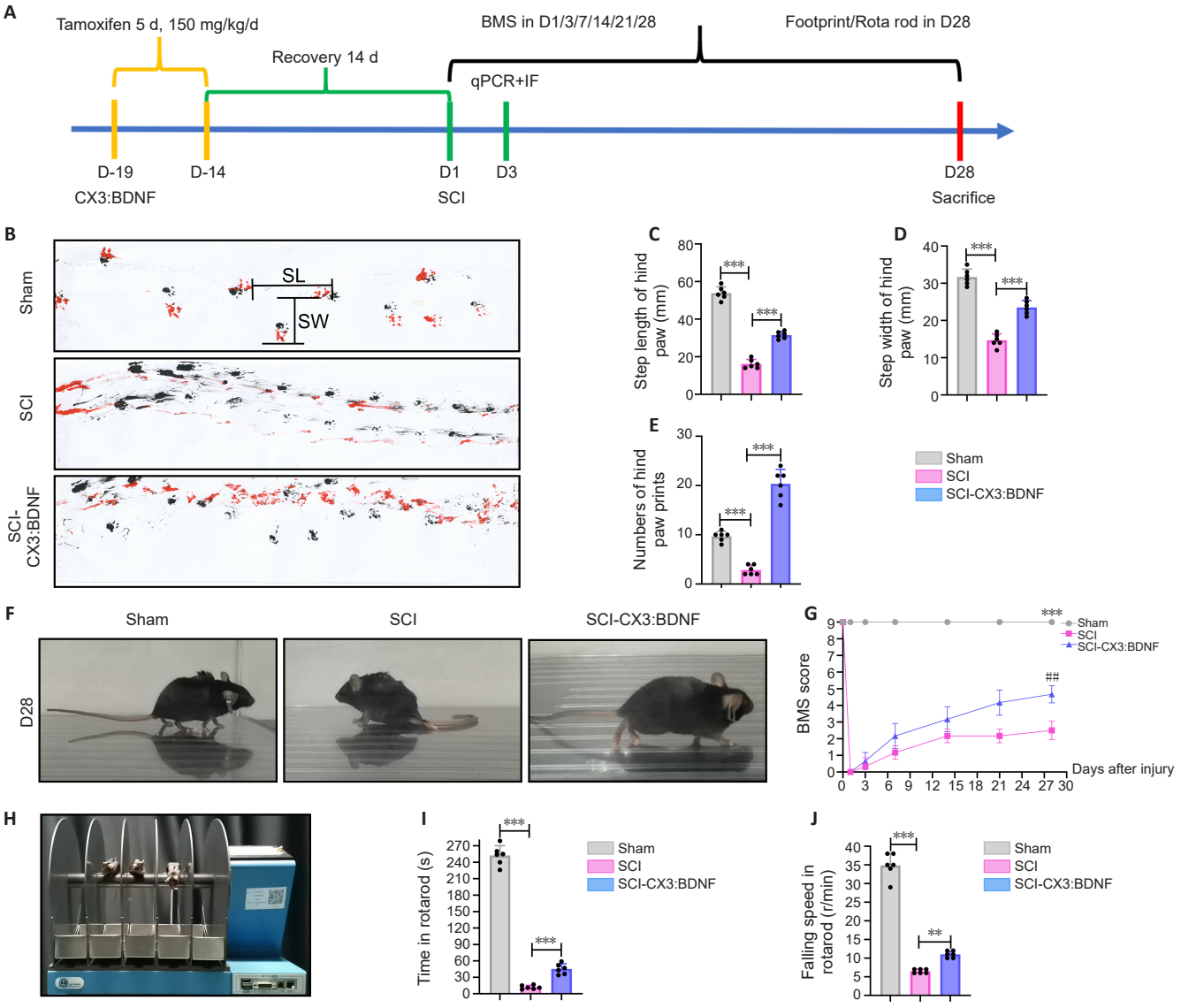

Figure 3 | **BDNF overexpression improves motor function.**

(A) Experimental timeline of spinal cord injury in CX3:BDNF mice. (B–E) Footprint analysis on day 28 post-spinal cord injury (SL, step length; SW, step width). (F, G) Microglial BDNF overexpression promotes motor function recovery after spinal cord injury, based on BMS scores (***P < 0.001, sham group *vs.* SCI group; ##P < 0.01, SCI group *vs.* SCI-CX3:BDNF group). (H–J) Rotarod analysis on day 28 post-spinal cord injury. One-way analysis of variance with Bonferroni *post hoc* test (C, D, E, I, J). Two-way repeated-measures analysis of variance with Bonferroni *post hoc* test (G). **P < 0.01, ***P < 0.001. In B–J, C57BL/6J mice were used in the Sham group and SCI group, and CX3:BDNF mice were used in SCI-CX3:BDNF group, and there were six mice in each group. BDNF: Brain-derived neurotrophic factor; BMS: Basso mouse scale; D1: day 1; IF: immunofluorescence; r/min: revolutions per minute; SCI: spinal cord injury.

Brain-derived neurotrophic factor overexpression by microglia favors neuronal and axonal survival after spinal cord injury

To elucidate the mechanism by which microglial BDNF overexpression promotes the recovery of motor function after SCI, we initially assessed axon and neuron preservation, as well as the expression of pro-apoptotic factors, in mice following SCI using immunofluorescence and quantitative reverse transcription-polymerase chain reaction (**Figure 4A–H**). 5-Hydroxytryptamine (5-HT, serotonin)-positive axons are an important axon type in the spinal cord. The descending 5-HT positive axons in the spinal cord regulate muscle tone, movement and rhythm, as well as movement coordination through a central pattern generator. SCI interrupts the projections of 5-HT positive axons where the central pattern generator is located, resulting in severe motor impairment. To investigate the effect of BDNF overexpression on axons, we counted the number of 5-HT-positive axons on day 28 after SCI. BDNF overexpression by mouse microglia preserved 5-HT-positive axons on day 28 post-SCI (**Figure 4A**) and reduced the number of apoptotic neurons on day 1 post-SCI (**Figure 4B**, **C**, **F**, **G**, **Additional Figure 3B**). Furthermore, BDNF expression by microglia promoted production of the anti-apoptotic factor *Bcl-2* (**Figure 4H**) and inhibited production of the pro-apoptotic factors *Bax* and *Caspase-3* (**Figure 4D** and **E**). These results indicate that BDNF overexpression by microglia inhibits apoptosis.

Brain-derived neurotrophic factor overexpression promotes microglial transition to an anti-inflammatory phenotype

Numerous previous studies have indicated that M2-type microglia promote anti-inflammatory factor secretion and BDNF expression (Van den Bossche et al., 2016; Ge et al., 2021; Zhang et al., 2021). The classification of microglia into M1 and M2 subtypes is not sufficiently comprehensive (Paolicelli et al., 2022), but M1/M2 classification reveals that different types of microglia may play distinct roles in the pathology of SCI (Stratoulias et al., 2023). To investigate the impact of BDNF overexpression on microglial phenotype and the secretion of inflammatory factors following SCI, we used two classical microglial markers: the anti-inflammatory marker Arg1 and the pro-inflammatory marker IL-1β. Our findings demonstrated that BDNF overexpression by microglia promoted increased the proportion of Arg1-positive microglia and decreased the proportion of IL-1β-positive microglia after SCI (**Figure 5A**, **B**, **E**, and **F**). Additionally, BDNF overexpression by microglia attenuated the secretion of inflammatory factors and enhanced the production of anti-inflammatory factors on day 3 after SCI (**Figure 5C**, **D**, **G**, and **H**). Furthermore, BDNF overexpression by microglia stimulated microglial activation up to day 28 post-SCI (**Additional Figures 3D** and **5**). These results suggest that BDNF overexpression by microglia may promote SCI repair by regulating microglial phenotype. In addition, we found that, under normal

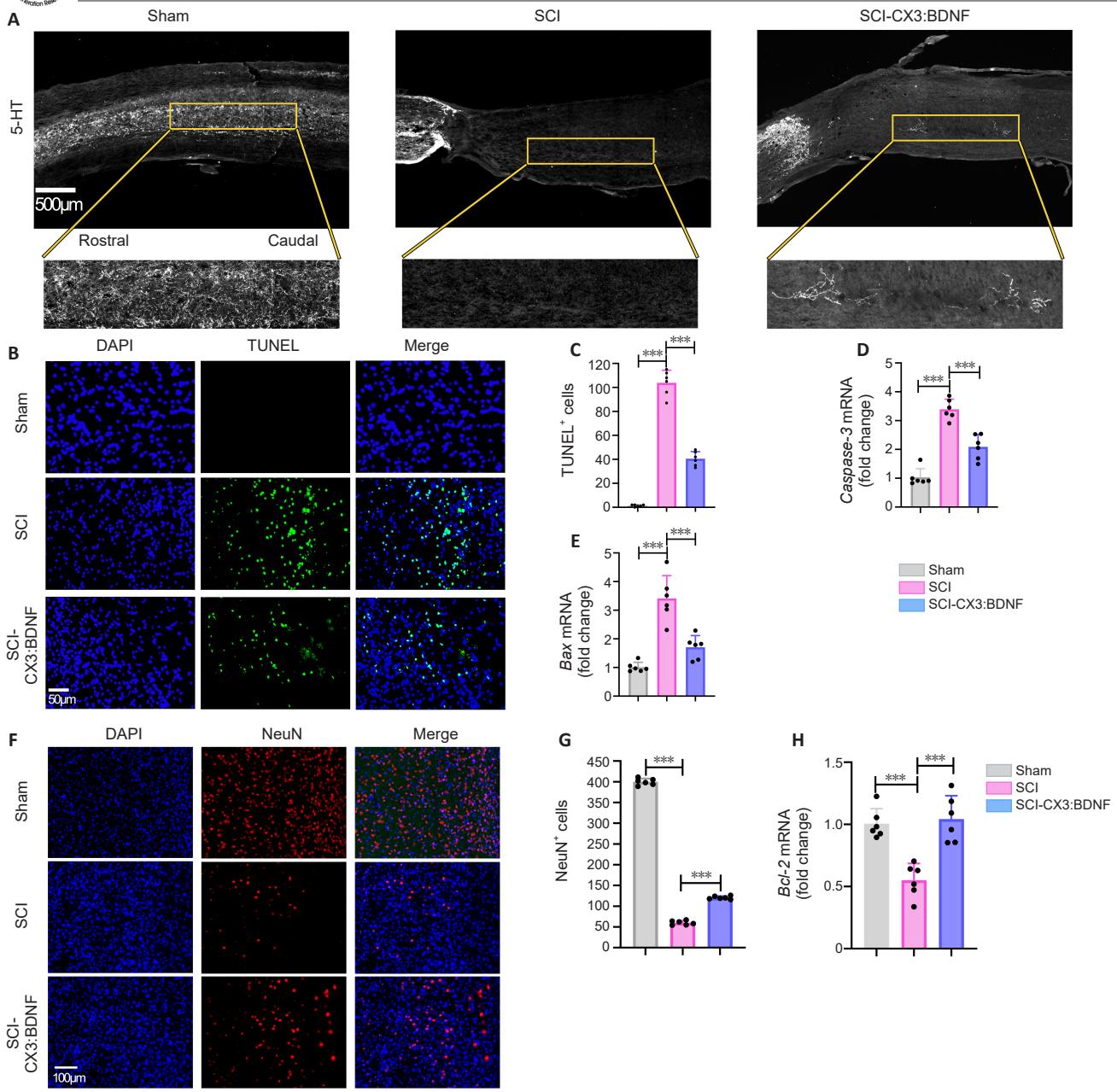

Figure 4 | **BDNF overexpression reduces neuronal apoptosis and axonal necrosis.**
(A) Immunofluorescence was employed to detect 5-HT-positive axons on day 28 post-spinal cord injury. Scale bar: 500 μm. 5-HT: white. (B–H) Microglial BDNF overexpression inhibits neuronal apoptosis following spinal cord injury. In B, scale bar: 50 μm, nuclei: blue, TUNEL: green. In F, scale bar: 100 μm, nuclei: blue, NeuN: red. One-way analysis of variance with Bonferroni *post hoc* test (C–E, G, H). Error bars in all figures represent SD. ***$P < 0.001$. In A–H, C57BL/6J mice were used in the sham and SCI groups, and CX3:BDNF mice were used in the SCI-CX3:BDNF group, and there were six mice in each group. BDNF: Brain-derived neurotrophic factor; DAPI: 4′,6-diamidino-2-phenylindole; 5-HT: 5-hydroxytryptamine; NeuN: neuronal nuclei; SCI: spinal cord injury; TUNEL: terminal deoxynucleotidyl transferase dUTP nick end labeling.

physiological conditions, BDNF overexpression did not affect the number and activation state of microglia, and that microglia overexpressing BDNF expressed the homeostatic marker P2RY12 and maintained a ramified morphology (**Figure 2C**). However, in the early stage after SCI, BNDF overexpression by microglia reduced the total number of activated microglia (**Figure 5**, 3 days post-SCI). In the late stage of SCI, BDNF overexpression increased the number of activated amoeboid microglia compared with the SCI group (**Figure 2E** and **Additional Figure 5**, 28 days post-SCI). Moreover, BDNF overexpression by microglia after SCI promotes microglial transition to an activated amoeboid Arg1-positive type. Our results indicate that BDNF overexpression by microglia reduces neuroinflammation and induces microglial phenotype transition.

Brain-derived neurotrophic factor overexpression promotes angiogenesis after spinal cord injury

SCI often disrupts the blood–spinal cord barrier, resulting in extensive hemorrhage, vascular rupture, and hematoma in the affected area, leading to destruction of the neurovascular network. Vascular cells play a crucial role in promoting the proliferation of neural precursor cells, and dividing cells are closely associated with blood vessels in the SGZ region of adult mice. Therefore, promoting reconstruction of the neurovascular network following SCI may be an effective strategy for treating this condition (Leventhal et al., 1999; Kojima et al., 2010; Tsai et al., 2016). Previous *in vitro* experiments have demonstrated that BDNF can promote blood vessel formation in vascular endothelial cells *in vitro* (Lin et al., 2014), and in this study, we assessed vascularization on day 28 after SCI through immunofluorescence staining. In the sham-operated group, opening the vertebral plates of mice did not have a large effect on blood flow to the mouse spinal cord, whereas a clamp injury resulted in a rapid disruption of blood flow to the mouse spinal cord (**Figure 6C–E**). Our findings revealed that BDNF overexpression by microglia effectively promoted blood vessel formation and increased blood flow compared with the SCI group following SCI (**Figure 6A–F**). Vessel density and blood flow were also increased, possibly due to the hypoxic environment that develops after SCI, which promotes hypoxia-inducible factor 1 secretion, subsequently stimulating blood vessel formation.

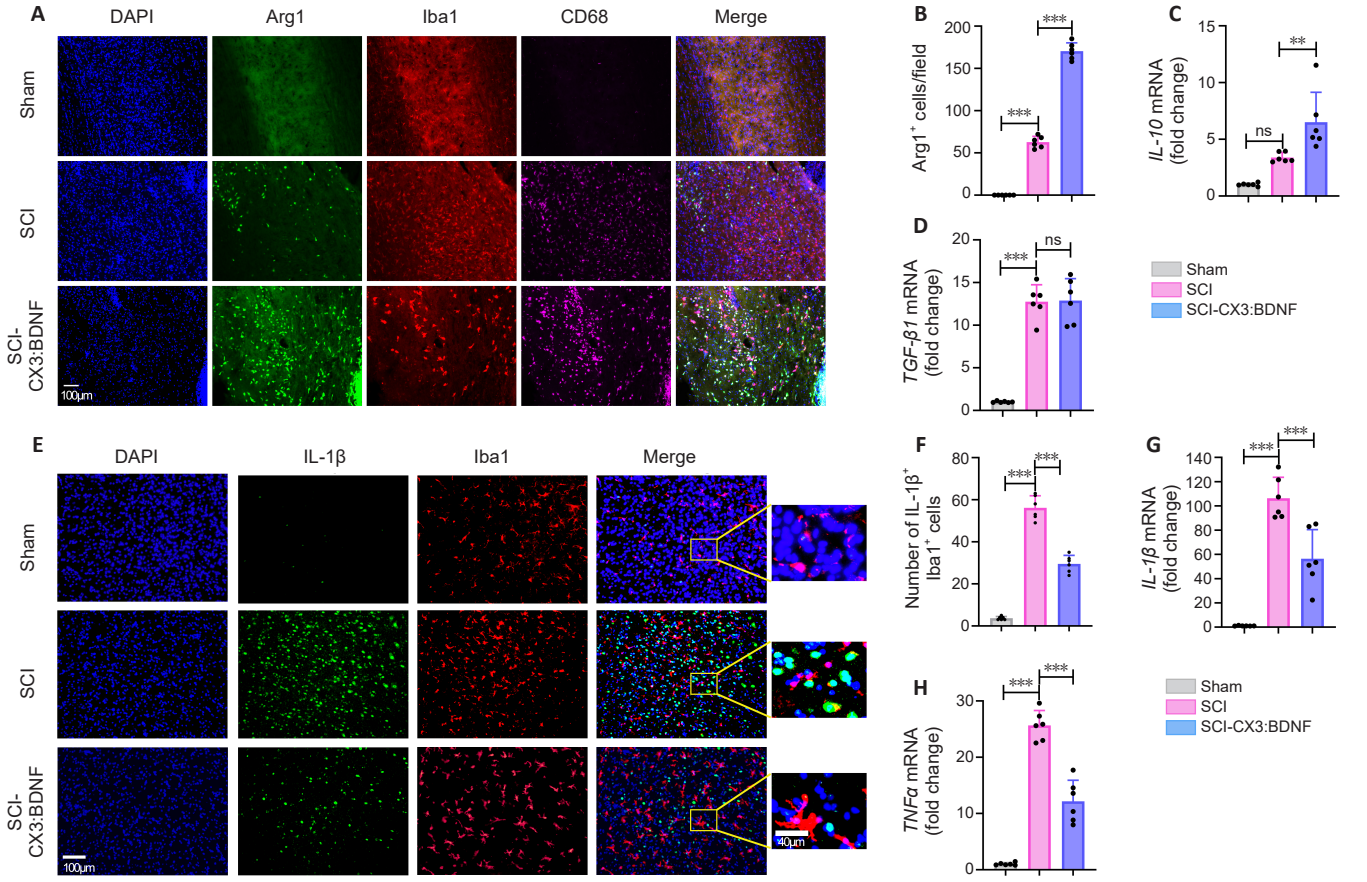

Figure 5 | **BDNF overexpression promotes activation of microglia to the Arg1-positive phenotype and reduces inflammation after spinal cord injury.**
(A–D) BDNF overexpression by microglia facilitates adoption of an anti-inflammatory type and enhances the production of anti-inflammatory factors on day 3 after spinal cord injury. Scale bar: 100 μm. Scale bar in enlarged figures: 40 μm. Nuclei: blue, Arg1: green, Iba1: red, CD68: magenta. (E–H) BDNF overexpression by microglia reduces the proportion of pro-inflammatory microglia and diminishes the production of pro-inflammatory factors on day 3 after spinal cord injury. Scale bar: 100 μm. Nuclei: blue, IL-1β: green, Iba1: red. One-way analysis of variance with Bonferroni *post hoc* test (B–D, F–H). $^{**}P < 0.01$, $^{***}P < 0.001$. In A–H, C57BL/6J mice were used in the Sham group and the SCI group, and CX3:BDNF mice were used in the SCI-CX3:BDNF group, and there were six mice in each group. BDNF: Brain-derived neurotrophic factor; DAPI: 4′,6-diamidino-2-phenylindole; SCI: spinal cord injury; IL-10: interleukin-10; IL-1β, interleukin-1β; ns: not significant; TGF-β1: transforming growth factor β1.

It has also been demonstrated in the previous study that the removal of microglia affects vascular regeneration after SCI (Li et al., 2020). Furthermore, we analyzed the association of BDNF with angiogenesis-related factors using Genemania and found strong associations and interactions between BDNF, VEGFA, Angpt1 (**Additional Figure 3E**). Subsequently, we examined VEGFA expression on the third day after SCI using qPCR and observed that BDNF overexpression by microglia promoted *VEGFA* expression following SCI (**Figure 6G**). These findings suggest that BDNF overexpression by microglia may promote angiogenesis and increase blood flow after SCI by enhancing *VEGFA* expression.

Primarily microglia, not macrophages, overexpress brain-derived neurotrophic factor to promote functional recovery from spinal cord injury

Both microglia and macrophages are labeled in the transgenic mice used in this experiment (CX3CR1 creER). It is worth noting that macrophages, which overexpress BDNF in the periphery following SCI, infiltrate toward the injury site (Bruttger et al., 2015). This raises the question of whether it is microglia or macrophages overexpressing BDNF that contribute to recovery after SCI. To address this, we employed the transgenic mouse line TMEM119 creER, in which microglia are labeled, as TMEM119 is expressed exclusively in microglia and not in macrophages (Bennett et al., 2016; Masuda et al., 2020). By crossing TMEM119 creER$^{+/+}$ mice with LSL-BDNF-tdTomato$^{+/+}$ mice, we obtained transgenic mice that specifically overexpress BDNF only in microglia (**Figure 7A**).

Initially, we assessed the labeling efficiency after tamoxifen gavage in the resulting transgenic mice and observed that the labeling efficiency in TMEM119 creER$^{-/+}$:LSL-BDNF$^{-/+}$- tdtomato mice was considerably lower than that in CX3CR1 creER mice (**Figure 7C**, **F** and **Additional Figure 3C**). Despite the low labelling efficiency of TMEM119 transgenic mice, overexpression of BDNF specifically in this fraction of labelled microglia was still able to facilitated the restoration of motor function in mice subjected to SCI (**Figure 7I**). To exclude the potential impact of peripheral macrophages, which also overexpress BDNF and infiltrate into the peripheral injury zone after SCI on SCI recovery. We administered dietary PLX73086 to the CX3:BDNF mice from 19 days prior to SCI until the 28th day after injury (**Figure 7B**). PLX73086 is a CSF1R inhibitor that have a low blood–brain barrier penetration. Our findings revealed that PLX73086 cleared macrophages from the peripheral liver, but did not clear microglia from the spinal cord (**Figure 7D**, **E**, **G**, and **H**), and that motor function was restored in CX3:BDNF mice treated with PLX73086 (**Figure 7J**). In summary, our findings suggest that it is primarily microglia overexpressing BDNF that play a therapeutic role in SCI.

Discussion

Microglia, as the most important immune cells in the CNS, play a crucial role in the pathology of SCI (David and Kroner, 2011; Zhou et al., 2020; Hakim et al., 2021). However, the precise role that microglia play in SCI, and the underlying mechanism, remain unclear, with conflicting opinions on whether microglia are beneficial or harmful in this context. To elucidate the role of microglia in SCI, we employed a mouse model in which microglia were completely removed by treatment with PLX5622 starting 14 days before injury and continuing until day 28 after injury. While sustained clearance of microglia has been shown to be detrimental to recovery from SCI, the underlying mechanism remains unknown. Our findings align with those of another study that demonstrates that complete removal of microglia is detrimental to recovery from SCI (Fu et al., 2020). Furthermore, our results suggest that microglia may play a protective role in the context of SCI by influencing astrocyte proliferation and regulating neuronal survival through the production of BDNF. However, it has also been reported microglia removal promotes recovery from SCI. Ma et al. (2020) used hydrogel-loaded PLX3397 to remove microglia from the spinal cord after SCI, then deactivated

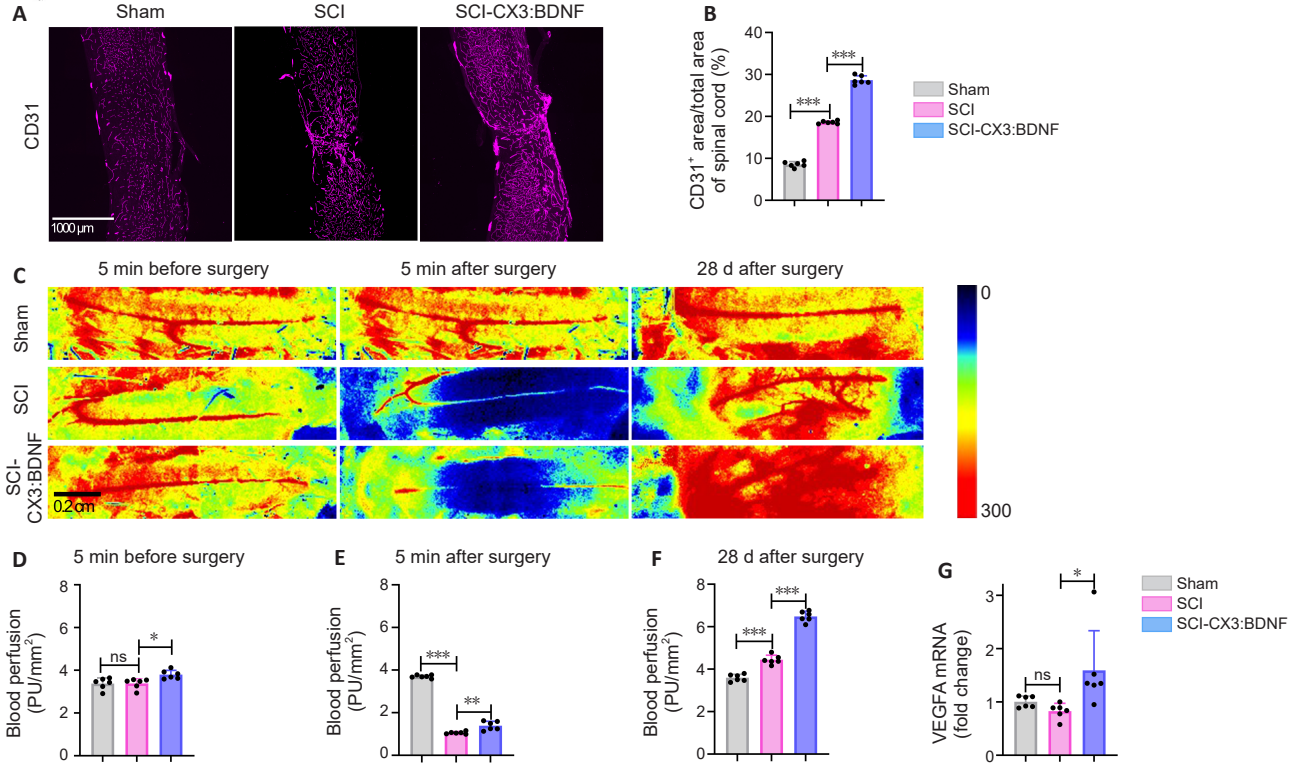

Figure 6 | **BDNF overexpression by microglia promotes vascular regeneration.**
(A, B) Blood vessel density on day 28 after spinal cord injury. Scale bar: 1000 μm. CD31: magenta. (C–F) Changes in blood flow before and after spinal cord injury. Scale bar: 0.2 cm. Low blood flow: blue, high blood flow: red. (G) VEGFA mRNA expression was detected on the third day after spinal cord injury. One-way analysis of variance with Bonferroni *post hoc* test (B, D–G). *P < 0.05, **P < 0.01, ***P < 0.001. In A–G, C57BL/6J mice were used in the Sham and SCI groups, and CX3:BDNF mice were used in the SCI-CX3:BDNF group, and there were six mice in each group. BDNF: Brain-derived neurotrophic factor; ns: not significant; SCI: spinal cord injury; VEGF: vascular endothelial growth factor.

PLX3397 on day 14 after injury, and observed a reduction in the production of inflammatory factors and an increase in the number of tuj1-positive neurons at the injury site. This suggests that microglia may have different functions at different stages of SCI. For instance, immediately after SCI, activated microglia release inflammatory factors that contribute to phagocytosis and clearance of necrotic endothelial and astrocytes, leading to disruption of the blood–spinal cord barrier (Figley et al., 2014). However, on the third day after SCI, microglia also release factors such as BDNF that promote recovery from SCI. Given the difficulty in infecting *in vivo* microglia with viruses, targeted delivery of exogenous genes or genetic modifications to microglia remains challenging. However, an alternative strategy of microglia transplantation proposed by Professor Peng Bo of Fudan University holds promise for treating a variety of CNS disease (Xu et al., 2020). Specifically, these strategies involve the use of a CSF1R inhibitor, based on traditional bone marrow transplantation, to remove microglia from the CNS, creating space for the transplanted cells to proliferate (Xu et al., 2021). Subsequently, peripheral bone marrow cells are used to replace the microglia in the CNS. Thus, therapeutic effects can be exerted by carrying therapeutic genes into the CNS after gene editing microglia or macrophages *in vitro*.

Although microglia removal during the inflammatory burst after SCI may be beneficial (Henry et al., 2020; Jakovcevski et al., 2021), the repair process after SCI relies heavily on microglial involvement. Furthermore, we observed that removing microglia resulted in downregulation of BDNF, which was unexpected, considering that microglia are not the primary BDNF-producing cells in the CNS. This suggests that BDNF derived from microglia plays a crucial role in recovery from SCI. Additionally, we found that expression of the anti-inflammatory factor transforming growth factor β1 was markedly increased in both the SCI group and the SCI-CX3:BDNF group when compared to the sham group, indicating a dynamic balance in the spinal cord microenvironment after SCI. Although anti-inflammatory factors were also upregulated in the SCI–WT group, the proportion of pro-inflammatory factors was higher, resulting in an overall pro-inflammatory phenotype. In an effort to identify the cell type responsible for promoting recovery from SCI through BDNF overexpression, we used mice in which microglia were specifically labeled. However, the functional recovery in this group was not as robust as that seen in the CX3:BDNF group, likely due to differences in labeling efficiency between the CX3CR1 creER and TMEM119 creER mouse lines.

The limitations of our research mainly lie in the fact that, although we found that microglia-derived BDNF is important for recovery from SCI, it remains unclear whether BDNF produced by different cell types plays different roles. Second, although we found that BDNF promotes vascular regeneration and upregulates VEGFA expression, the specific mechanism still needs to be investigated. In conclusion, our study demonstrates that sustained removal of microglia leads to a decrease in BDNF levels and hinders recovery from SCI. Microglia can influence recovery from SCI by regulating astrocyte proliferation and neuronal survival. Furthermore, BDNF overexpression by microglia promotes angiogenesis and induces microglia phenotype transition. Our *in vivo* experiments demonstrated that BDNF overexpression by microglia upregulates VEGFA expression and promotes vascular regeneration after SCI, thereby increasing blood flow to the spinal cord. This may benefit neuronal survival and reconstruction of the neurovascular network. Inducing microglia to overexpress BDNF may therefore represent an effective strategy for treating SCI.

Acknowledgments: *We extend our gratitude to Professor Bo Peng of Fudan University for generously providing genetically modified mice, PLX5622 and PLX73086, as well as for his support and assistance in this experiment. We also acknowledge the public platform of Fudan University Brain Science Translation Institute and the Central Laboratory of Xiangyang Central Hospital for the support of this project. The schema chart was primarily created using PowerPoint and Figdraw (www.figdraw.com).*
Author contributions: *XM and FZ designed this study. FZ wrote the manuscript and performed the experiments. YL, XL, and SC participated in part of the experiments. XG and YC assisted in breeding and caring for genetically modified mice. FZ, YL, and XL analyzed the data. XM, RM, and HT sponsored and supervised the project. All authors approved the final version of the paper.*
Conflicts of interest: *The authors declare that they have no known competing financial interests or personal relationships that could have appeared to influence the work reported in this paper.*
Data availability statement: *The datasets during and analyzed during the current study available from the corresponding author on reasonable request.*

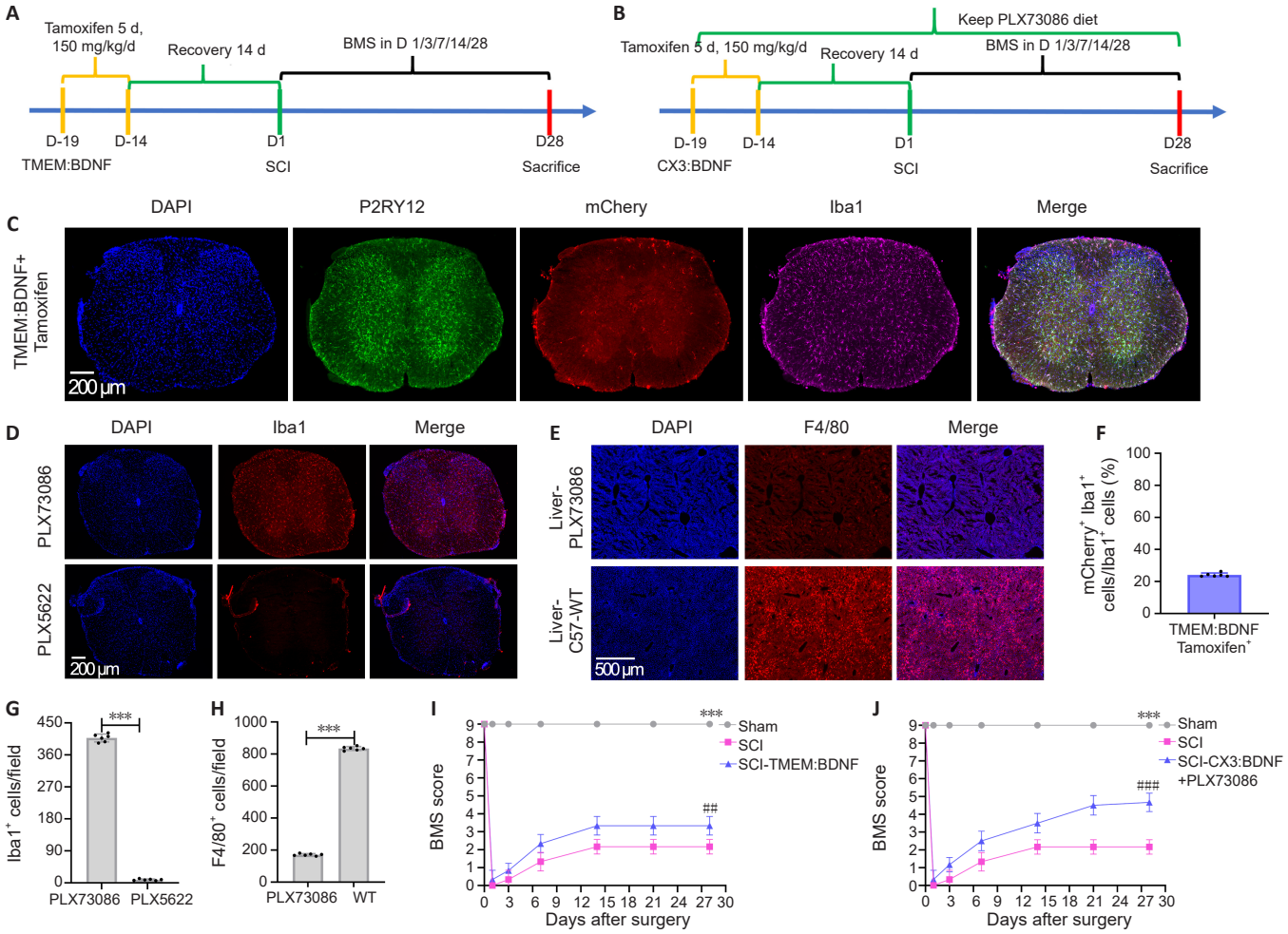

Figure 7 | **BDNF overexpression primarily by microglia but not by macrophages promotes functional recovery after spinal cord injury.**

(A, B) Experimental timeline of spinal cord injury in TMEM:BDNF mice and CX3:BDNF + PLX73086 mice. (C, F) Detection of induction efficiency in TMEM:BDNF mice. Scale bar: 200 μm. Nuclei: blue, P2RY12: green, mCherry (mCherry is used to label tdTomato proteins, a red fluorescent protein. mCherry labelled cells here are mainly TMEM119 positive cells): red, Iba1: magenta. (D, G) Unlike PLX5622, PLX73086 did not affect the number of microglia in the spinal cord. Scale bar: 200 μm. DAPI: Blue, Iba1: Red. (E, H) PLX73086 exhibits effective scavenging of peripheral macrophages. Scale bar: 500 μm. Nuclei: blue, F4/80: red. (I, J) BMS scores after spinal cord injury in the TMEM:BDNF and CX3:BDNF + PLX73086 groups (I, ***P < 0.001, sham group *vs.* SCI group. ###P < 0.01, SCI group *vs.* SCI-TMEM:BDNF group; J, ***P < 0.001, sham group *vs.* SCI group. ###P < 0.001, SCI group *vs.* SCI-CX3:BDNF + PLX73086 group). Mean ± SD (F). Unpaired *t*-test (G, H). Two-way repeated-measures analysis of variance with Bonferroni *post hoc* test (I, J). ***P < 0.001 in G. The mice used in C and F were TMEM:BDNF, and there were six mice in each group. The mice used in D, E, G, H, and F were C57BL/6J mice, and there were six mice in each group. In Figure I, C57BL/6J mice were used in the Sham group, SCI group, and WT group, and CX3:BDNF mice were used in the SCI-TMEM:BDNF group, and there were six mice in each group. In Figure J, C57BL/6J mice were used in the Sham, SCI, and WT groups, and CX3:BDNF mice were used in the SCI-CX3:BDNF + PLX73086 group, and there were six mice in each group. BDNF: Brain-derived neurotrophic factor; DAPI: 4',6-diamidino-2-phenylindole; D1: day 1; SCI: spinal cord injury.

Additional files:

Additional Figure 1: *Experimental flowchart.*

Additional Figure 2: *Gene identification.*

Additional Figure 3: *Correlation analysis of BDNF and angiogenesis.*

Additional Figure 4: *Removal of microglia increases lesion size after spinal cord injury.*

Additional Figure 5: *BDNF overexpression by microglia resulted in sustained activation of microglia on day 28 after spinal cord injury.*

Additional Table 1: *Sequences of primers used for genotyping.*

Additional Table 2: *Sequences of primers used for quantitative reverse transcription-polymerase chain reaction.*

References

Anderson MA, Squair JW, Gautier M, Hutson TH, Kathe C, Barraud Q, Bloch J, Courtine G (2022) Natural and targeted circuit reorganization after spinal cord injury. Nat Neurosci 25:1584-1596.

Barde YA, Edgar D, Thoenen H (1982) Purification of a new neurotrophic factor from mammalian brain. EMBO J 1:549-553.

Basso DM, Fisher LC, Anderson AJ, Jakeman LB, McTigue DM, Popovich PG (2006) Basso Mouse Scale for locomotion detects differences in recovery after spinal cord injury in five common mouse strains. J Neurotrauma 23:635-659.

Bathina S, Das UN (2015) Brain-derived neurotrophic factor and its clinical implications. Arch Med Sci 11:1164-1178.

Bellver-Landete V, Bretheau F, Mailhot B, Vallieres N, Lessard M, Janelle ME, Vernoux N, Tremblay ME, Fuehrmann T, Shoichet MS, Lacroix S (2019) Microglia are an essential component of the neuroprotective scar that forms after spinal cord injury. Nat Commun 10:518.

Bennett ML, Bennett FC, Liddelow SA, Ajami B, Zamanian JL, Fernhoff NB, Mulinyawe SB, Bohlen CJ, Adil A, Tucker A, Weissman IL, Chang EF, Li G, Grant GA, Hayden Gephart MG, Barres BA (2016) New tools for studying microglia in the mouse and human CNS. Proc Natl Acad Sci U S A 113:E1738-1746.

Borst K, Dumas AA, Prinz M (2021) Microglia: Immune and non-immune functions. Immunity 54:2194-2208.

Bradbury EJ, Moon LD, Popat RJ, King VR, Bennett GS, Patel PN, Fawcett JW, McMahon SB (2002) Chondroitinase ABC promotes functional recovery after spinal cord injury. Nature 416:636-640.

Brennan FH, Li Y, Wang C, Ma A, Guo Q, Li Y, Pukos N, Campbell WA, Witcher KG, Guan Z, Kigerl KA, Hall JCE, Godbout JP, Fischer AJ, McTigue DM, He Z, Ma Q, Popovich PG (2022) Microglia coordinate cellular interactions during spinal cord repair in mice. Nat Commun 13:4096.

Brockie S, Zhou C, Fehlings MG (2024) Resident immune responses to spinal cord injury: role of astrocytes and microglia. Neural Regen Res 19:1678-1685.

Bruttger J, Karram K, Wortge S, Regen T, Marini F, Hoppmann N, Klein M, Blank T, Yona S, Wolf Y, Mack M, Pinteaux E, Muller W, Zipp F, Binder H, Bopp T, Prinz M, Jung S, Waisman A (2015) Genetic cell ablation reveals clusters of local self-renewing microglia in the mammalian central nervous system. Immunity 43:92-106.

Butovsky O, Weiner HL (2018) Microglial signatures and their role in health and disease. Nat Rev Neurosci 19:622-635.

Castro-Gomez S, Heneka MT (2024) Innate immune activation in neurodegenerative diseases. Immunity 57:790-814.

Chao MV, Hempstead BL (1995) p75 and Trk: a two-receptor system. Trends Neurosci 18:321-326.

Cheng Q, Song SH, Augustine GJ (2017) Calcium-dependent and synapsin-dependent pathways for the presynaptic actions of BDNF. Front Cell Neurosci 11:75.

Chiang CY, Sessle BJ, Dostrovsky JO (2012) Role of astrocytes in pain. Neurochem Res 37:2419-2431.

Colonna M, Butovsky O (2017) Microglia function in the central nervous system during health and neurodegeneration. Annu Rev Immunol 35:441-468.

David S, Kroner A (2011) Repertoire of microglial and macrophage responses after spinal cord injury. Nat Rev Neurosci 12:388-399.
Egan MF, Kojima M, Callicott JH, Goldberg TE, Kolachana BS, Bertolino A, Zaitsev E, Gold B, Goldman D, Dean M, Lu B, Weinberger DR (2003) The BDNF val66met polymorphism affects activity-dependent secretion of BDNF and human memory and hippocampal function. Cell 112:257-269.
Elmore MR, Najafi AR, Koike MA, Dagher NN, Spangenberg EE, Rice RA, Kitazawa M, Matusow B, Nguyen H, West BL, Green KN (2014) Colony-stimulating factor 1 receptor signaling is necessary for microglia viability, unmasking a microglia progenitor cell in the adult brain. Neuron 82:380-397.
Fan Z, Jia M, Zhou J, Zhu Z, Wu Y, Lin X, Qian Y, Lian J, Hua X, Dong J, Fang Z, Liu Y, Chen S, Xue X, Yue J, Zhu M, Wang Y, Huang Z, Teng H (2024) Pharmacological targeting cGAS/STING/NF-κB axis by tryptanthrin induces microglia polarization toward M2 phenotype and promotes functional recovery in a mouse model of spinal cord injury. Neural Regen Res doi: 10.4103/NRR.NRR-D-23-01256.
Fang S, Zhong L, Wang AQ, Zhang H, Yin ZS (2021) Identification of regeneration and hub genes and pathways at different time points after spinal cord injury. Mol Neurobiol 58:2643-2662.
Figley SA, Khosravi R, Legasto JM, Tseng YF, Fehlings MG (2014) Characterization of vascular disruption and blood-spinal cord barrier permeability following traumatic spinal cord injury. J Neurotrauma 31:541-552.
Fu H, Zhao Y, Hu D, Wang S, Yu T, Zhang L (2020) Depletion of microglia exacerbates injury and impairs function recovery after spinal cord injury in mice. Cell Death Dis 11:528.
Ge X, et al. (2021) Exosomal miR-155 from M1-polarized macrophages promotes EndoMT and impairs mitochondrial function via activating NF-kappaB signaling pathway in vascular endothelial cells after traumatic spinal cord injury. Redox Biol 41:101932.
Ginhoux F, Greter M, Leboeuf M, Nandi S, See P, Gokhan S, Mehler MF, Conway SJ, Ng LG, Stanley ER, Samokhvalov IM, Merad M (2010) Fate mapping analysis reveals that adult microglia derive from primitive macrophages. Science 330:841-845.
Gong L, Gu Y, Han X, Luan C, Liu C, Wang X, Sun Y, Zheng M, Fang M, Yang S, Xu L, Sun H, Yu B, Gu X, Zhou S (2023) Spatiotemporal dynamics of the molecular expression pattern and intercellular interactions in the glial scar response to spinal cord injury. Neurosci Bull 39:213-244.
Hakim R, Zachariadis V, Sankavaram SR, Han J, Harris RA, Brundin L, Enge M, Svensson M (2021) Spinal cord injury induces permanent reprogramming of microglia into a disease-associated state which contributes to functional recovery. J Neurosci 41:8441-8459.
Henry RJ, Ritzel RM, Barrett JP, Doran SJ, Jiao Y, Leach JB, Szeto GL, Wu J, Stoica BA, Faden AI, Loane DJ (2020) Microglial depletion with CSF1R inhibitor during chronic phase of experimental traumatic brain injury reduces neurodegeneration and neurological deficits. J Neurosci 40:2960-2974.
Jakovcevski I, Forster E, Reiss G, Schachner M (2021) Impact of depletion of microglia/macrophages on regeneration after spinal cord injury. Neuroscience 459:129-141.
Kierdorf K et al. (2013) Microglia emerge from erythromyeloid precursors via Pu.1- and Irf8-dependent pathways. Nat Neurosci 16:273-280.
Kojima T, Hirota Y, Ema M, Takahashi S, Miyoshi I, Okano H, Sawamoto K (2010) Subventricular zone-derived neural progenitor cells migrate along a blood vessel scaffold toward the post-stroke striatum. Stem Cells 28:545-554.
Kunkel-Bagden E, Dai HN, Bregman BS (1993) Methods to assess the development and recovery of locomotor function after spinal cord injury in rats. Exp Neurol 119:153-164.
Lee BB, Cripps RA, Fitzharris M, Wing PC (2014) The global map for traumatic spinal cord injury epidemiology: update 2011, global incidence rate. Spinal Cord 52:110-116.
Lessmann V, Brigadski T (2009) Mechanisms, locations, and kinetics of synaptic BDNF secretion: an update. Neurosci Res 65:11-22.
Leventhal C, Rafii S, Rafii D, Shahar A, Goldman SA (1999) Endothelial trophic support of neuronal production and recruitment from the adult mammalian subependyma. Mol Cell Neurosci 13:450-464.
Li C, Wu Z, Zhou L, Shao J, Hu X, Xu W, Ren Y, Zhu X, Ge W, Zhang K, Liu J, Huang R, Yu J, Luo D, Yang X, Zhu W, Zhu R, Zheng C, Sun YE, Cheng L (2022a) Temporal and spatial cellular and molecular pathological alterations with single-cell resolution in the adult spinal cord after injury. Signal Transduct Target Ther 7:65.
Li F, Sun X, Sun K, Kong F, Jiang X, Kong Q (2024) Lupenone improves motor dysfunction in spinal cord injury mice through inhibiting the inflammasome activation and pyroptosis in microglia via the nuclear factor kappa B pathway. Neural Regen Res 19:1802-1811.
Li Y, Lei Z, Ritzel RM, He J, Li H, Choi HMC, Lipinski MM, Wu J (2022b) Impairment of autophagy after spinal cord injury potentiates neuroinflammation and motor function deficit in mice. Theranostics 12:5364-5388.
Li Y, He X, Kawaguchi R, Zhang Y, Wang Q, Monavarfeshani A, Yang Z, Chen B, Shi Z, Meng H, Zhou S, Zhu J, Jacobi A, Swarup V, Popovich PG, Geschwind DH, He Z (2020) Microglia-organized scar-free spinal cord repair in neonatal mice. Nature 587:613-618.
Lima Giacobbo B, Doorduin J, Klein HC, Dierckx R, Bromberg E, de Vries EFJ (2019) Brain-derived neurotrophic factor in brain disorders: focus on neuroinflammation. Mol Neurobiol 56:3295-3312.
Lin CY, Hung SY, Chen HT, Tsou HK, Fong YC, Wang SW, Tang CH (2014) Brain-derived neurotrophic factor increases vascular endothelial growth factor expression and enhances angiogenesis in human chondrosarcoma cells. Biochem Pharmacol 91:522-533.
Liu XZ, Xu XM, Hu R, Du C, Zhang SX, McDonald JW, Dong HX, Wu YJ, Fan GS, Jacquin MF, Hsu CY, Choi DW (1997) Neuronal and glial apoptosis after traumatic spinal cord injury. J Neurosci 17:5395-5406.
Liu Y, Zhang B, Duan R, Liu Y (2024) Mitochondrial DNA leakage and cGas/STING pathway in microglia: crosstalk between neuroinflammation and neurodegeneration. Neuroscience 548:1-8.
Liu Z, Yao X, Jiang W, Li W, Zhu S, Liao C, Zou L, Ding R, Chen J (2020) Advanced oxidation protein products induce microglia-mediated neuroinflammation via MAPKs-NF-kappaB signaling pathway and pyroptosis after secondary spinal cord injury. J Neuroinflammation 17:90.
Ma D, Zhao Y, Huang L, Xiao Z, Chen B, Shi Y, Shen H, Dai J (2020) A novel hydrogel-based treatment for complete transection spinal cord injury repair is driven by microglia/macrophages repopulation. Biomaterials 237:119830.
Masuda T, Amann L, Sankowski R, Staszewski O, Lenz M, P DE, Snaidero N, Costa Jordao MJ, Bottcher C, Kierdorf K, Jung S, Priller J, Misgeld T, Vlachos A, Meyer-Luehmann M, Knobeloch KP, Prinz M (2020) Novel Hexb-based tools for studying microglia in the CNS. Nat Immunol 21:802-815.
Matson KJE, Russ DE, Kathe C, Hua I, Maric D, Ding Y, Krynitsky J, Pursley R, Sathyamurthy A, Squair JW, Levi BP, Courtine G, Levine AJ (2022) Single cell atlas of spinal cord injury in mice reveals a pro-regenerative signature in spinocerebellar neurons. Nat Commun 13:5628.
Meeker R, Williams K (2014) Dynamic nature of the p75 neurotrophin receptor in response to injury and disease. J Neuroimmune Pharmacol 9:615-628.
Mori A, Nishioka Y, Yamada M, Nishibata Y, Masuda S, Tomaru U, Honma N, Moriyama T, Ishizu A (2018) Brain-derived neurotrophic factor induces angiogenin secretion and nuclear translocation in human umbilical vein endothelial cells. Pathol Res Pract 214:521-526.
Mowla SJ, Farhadi HF, Pareek S, Atwal JK, Morris SJ, Seidah NG, Murphy RA (2001) Biosynthesis and post-translational processing of the precursor to brain-derived neurotrophic factor. J Biol Chem 276:12660-12666.
Pang QM, Chen SY, Xu QJ, Zhang M, Liang DF, Fu SP, Yu J, Liu ZL, Zhang Q, Zhang T (2022) Effects of astrocytes and microglia on neuroinflammation after spinal cord injury and related immunomodulatory strategies. Int Immunopharmacol 108:108754.
Paolicelli RC, et al. (2022) Microglia states and nomenclature: A field at its crossroads. Neuron 110:3458-3483.
Parkhurst CN, Yang G, Ninan I, Savas JN, Yates JR, 3rd, Lafaille JJ, Hempstead BL, Littman DR, Gan WB (2013) Microglia promote learning-dependent synapse formation through brain-derived neurotrophic factor. Cell 155:1596-1609.
Percie du Sert N, et al. (2020) The ARRIVE guidelines 2.0: Updated guidelines for reporting animal research. PLoS Biol 18:e3000410.
Prinz M, Jung S, Priller J (2019) Microglia biology: one century of evolving concepts. Cell 179:292-311.
Sasi M, Vignoli B, Canossa M, Blum R (2017) Neurobiology of local and intercellular BDNF signaling. Pflugers Arch 469:593-610.
Schneider CA, Rasband WS, Eliceiri KW (2012) NIH Image to ImageJ: 25 years of image analysis. Nat Methods 9:671-675.
Sierra A, Encinas JM, Deudero JJ, Chancey JH, Enikolopov G, Overstreet-Wadiche LS, Tsirka SE, Maletic-Savatic M (2010) Microglia shape adult hippocampal neurogenesis through apoptosis-coupled phagocytosis. Cell Stem Cell 7:483-495.
Smith PA (2014) BDNF: no gain without pain? Neuroscience 283:107-123.
Stratoulias V, et al. (2023) ARG1-expressing microglia show a distinct molecular signature and modulate postnatal development and function of the mouse brain. Nat Neurosci 26:1008-1020.
Tan L, Liang J, Wang X, Wang Y, Xiong T (2024) Dual roles of microglia in the pathological injury and repair of hemorrhagic cerebrovascular diseases. Regen Med Rep 1:93-105.
Tang H, Gu Y, Jiang L, Zheng G, Pan Z, Jiang X (2022) The role of immune cells and associated immunological factors in the immune response to spinal cord injury. Front Immunol 13:1070540.
Tang Y, Le W (2016) Differential roles of M1 and M2 microglia in neurodegenerative diseases. Mol Neurobiol 53:1181-1194.
Tsai HH, Niu J, Munji R, Davalos D, Chang J, Zhang H, Tien AC, Kuo CJ, Chan JR, Daneman R, Fancy SP (2016) Oligodendrocyte precursors migrate along vasculature in the developing nervous system. Science 351:379-384.
Tsuda M, Inoue K, Salter MW (2005) Neuropathic pain and spinal microglia: a big problem from molecules in "small" glia. Trends Neurosci 28:101-107.
Van den Bossche J, Baardman J, Otto NA, van der Velden S, Neele AE, van den Berg SM, Luque-Martin R, Chen HJ, Boshuizen MC, Ahmed M, Hoeksema MA, de Vos AF, de Winther MP (2016) Mitochondrial dysfunction prevents repolarization of inflammatory macrophages. Cell Rep 17:684-696.
Wang J, He W, Zhang J (2023a) A richer and more diverse future for microglia phenotypes. Heliyon 9:e14713.
Wang W, Li Y, Ma F, Sheng X, Chen K, Zhuo R, Wang C, Zheng H, Zhang YW, Bu G, Chen XF, Zhong L (2023b) Microglial repopulation reverses cognitive and synaptic deficits in an Alzheimer's disease model by restoring BDNF signaling. Brain Behav Immun 113:275-288.
Wang Z, Zhou W, Zhang Z, Zhang L, Li M (2024) Metformin alleviates spinal cord injury by inhibiting nerve cell ferroptosis through upregulation of heme oxygenase-1 expression. Neural Regen Res 19:2041-2049.
Willis EF, MacDonald KPA, Nguyen QH, Garrido AL, Gillespie ER, Harley SBR, Bartlett PF, Schroder WA, Yates AG, Anthony DC, Rose-John S, Ruitenberg MJ, Vukovic J (2020) Repopulating microglia promote brain repair in an IL-6-dependent manner. Cell 180:833-846 e816.
Xu Y, Geng Y, Wang H, Zhang H, Qi J, Li F, Hu X, Chen Y, Si H, Li Y, Wang X, Xu H, Kong J, Cai Y, Wu A, Ni W, Xiao J, Zhou K (2023) Cyclic helix B peptide alleviates proinflammatory cell death and improves functional recovery after traumatic spinal cord injury. Redox Biol 64:102767.
Xu Z, Zhou X, Peng B, Rao Y (2021) Microglia replacement by bone marrow transplantation (Mr BMT) in the central nervous system of adult mice. STAR Protoc 2:100666.
Xu Z, Rao Y, Huang Y, Zhou T, Feng R, Xiong S, Yuan TF, Qin S, Lu Y, Zhou X, Li X, Qin B, Mao Y, Peng B (2020) Efficient strategies for microglia replacement in the central nervous system. Cell Rep 32:108041.
Zeng F, Chen A, Chen W, Cheng S, Lin S, Mei R, Mei X (2024) Knockout of TNF-α in microglia decreases ferroptosis and convert microglia phenotype after spinal cord injury. Heliyon 10:e36488.
Zhang J, Rong P, Zhang L, He H, Zhou T, Fan Y, Mo L, Zhao Q, Han Y, Li S, Wang Y, Yan W, Chen H, You Z (2021) IL4-driven microglia modulate stress resilience through BDNF-dependent neurogenesis. Sci Adv 7.
Zhang Y, Chen K, Sloan SA, Bennett ML, Scholze AR, O'Keeffe S, Phatnani HP, Guarnieri P, Caneda C, Ruderisch N, Deng S, Liddelow SA, Zhang C, Daneman R, Maniatis T, Barres BA, Wu JQ (2014) An RNA-sequencing transcriptome and splicing database of glia, neurons, and vascular cells of the cerebral cortex. J Neurosci 34:11929-11947.
Zhou HY, Wang X, Li Y, Wang D, Zhou XZ, Xiao N, Li GX, Li G (2024) Dynamic development of microglia and macrophages after spinal cord injury. Neural Regen Res doi: 10.4103/NRR.NRR-D-24-00063.
Zhou W, Xie Z, Li C, Xing Z, Xie S, Li M, Yao J (2021) Driving effect of BDNF in the spinal dorsal horn on neuropathic pain. Neurosci Lett 756:135965.
Zhou X, Wahane S, Friedl MS, Kluge M, Friedel CC, Avrampou K, Zachariou V, Guo L, Zhang B, He X, Friedel RH, Zou H (2020) Microglia and macrophages promote corralling, wound compaction and recovery after spinal cord injury via Plexin-B2. Nat Neurosci 23:337-350.

C-Editor: Zhao M; S-Editor: Li CH; L-Editors: Li CH, Song LP; T-Editor: Jia Y

Additional figures

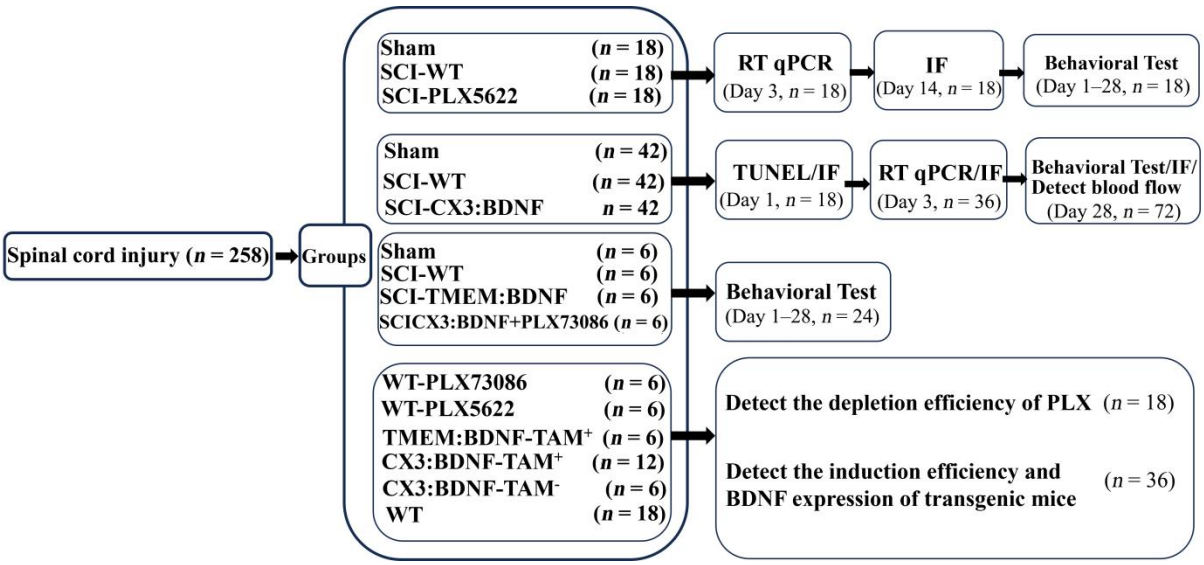

Additional Figure 1 Experimental flowchart.

BDNF: Brain-derived neurotrophic factor; IF: immunofluorescence; PLX73086 and PLX5622: colony-stimulating factor 1 receptor inhibitor; RT-qPCR: quantitative reverse transcription-polymerase chain reaction; SCI: spinal cord injury; TUNEL: terminal deoxynucleotidyl transferase dUTP nick end labeling; WT: wild-type.

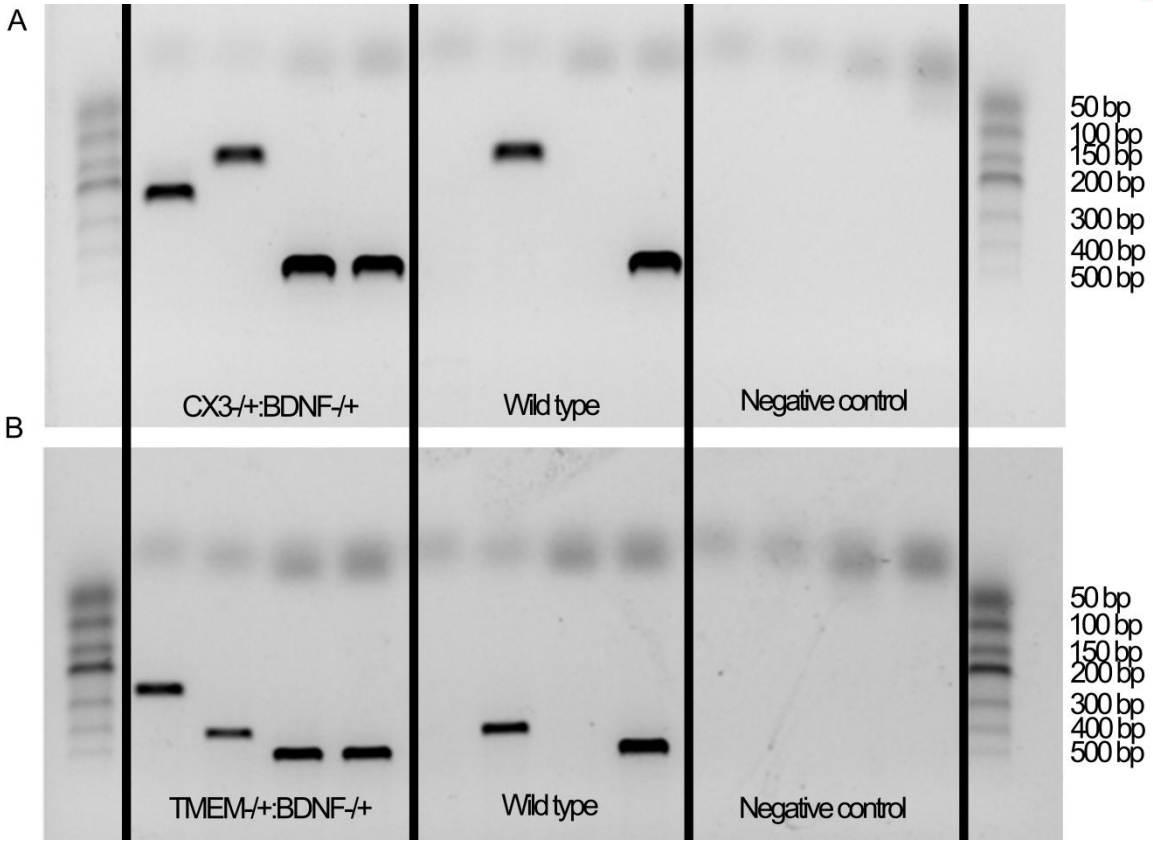

Additional Figure 2 Gene identification.

(A) Agarose gel electrophoresis analysis of CX3:BDNF transgenic mice. CX3CR1 creER wildtype, 151 bp. CX3CR1 creER mutant, 230 bp. BDNF wild-type, 469 bp. BDNF mutant, 475 bp. (B) Agarose gel electrophoresis analysis of TMEM:BDNF transgenic mice. TAKARA DL500 marker. TMEM119 creER wild-type, 378 bp. TMEM119 creER mutant, 280 bp. BDNF: Brain-derived neurotrophic factor.

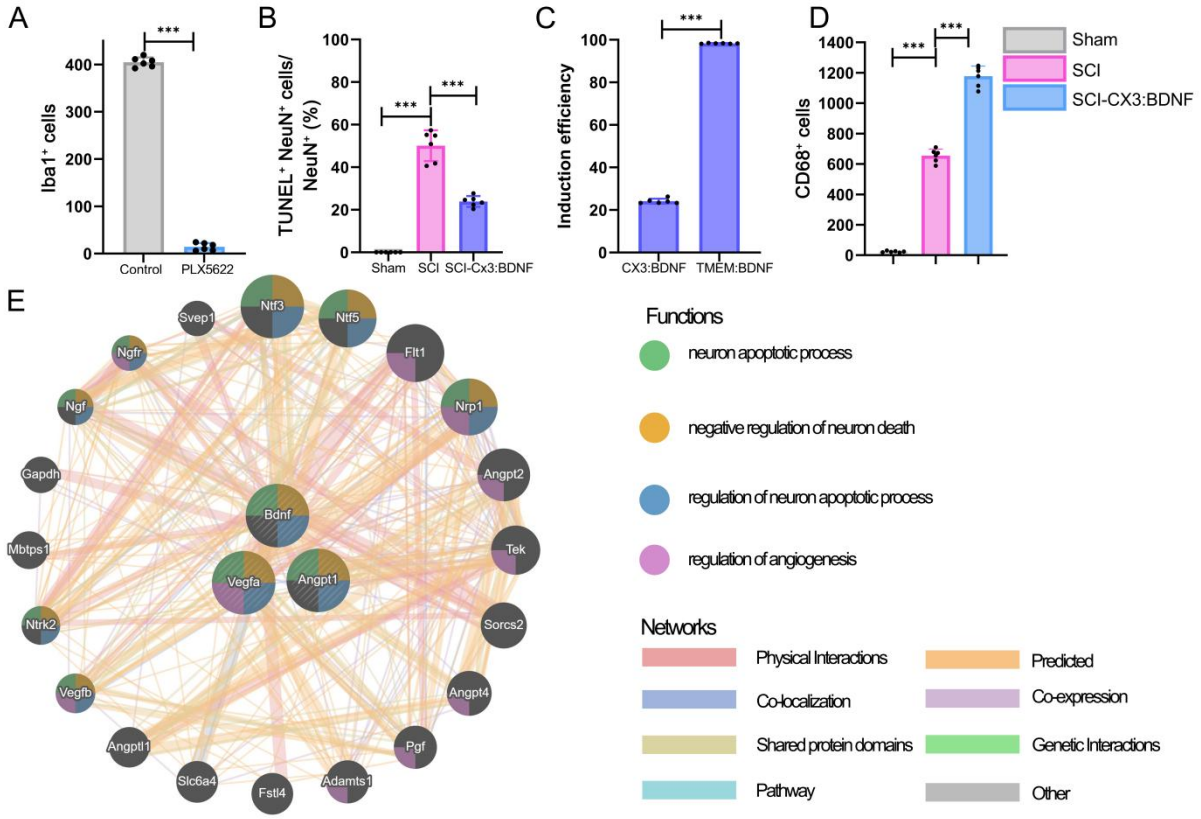

Additional Figure 3 Correlation analysis of BDNF and angiogenesis.

(A) Depletion efficiency of PLX5622. (B) BDNF overexpression by microglia can reduce neuronal apoptosis on day 1 of spinal cord injury, based on TUNEL experiments. (C) Comparison of the induction efficiency of microglia in TMEM:BDNF and CX3:BDNF mice. (D) The statistical results of CD68+ cells are supplemented in Additional Figure 5. Data shown are from 28 days after spinal cord injury. (E) The correlation between BDNF and angiogenesis was analyzed using Genemania. Student's unpaired t-test (A, C); one-way analysis of variance with Bonferroni post hoc test (B, D). *$P < 0.05$, ** $P < 0.01$, *** $P < 0.001$. In Additional Figure 1A, the mice were WT mice, and there were six mice in each group. In Additional Figure 1B and 1D, C57BL/6J mice were used in the sham and SCI groups, and CX3:BDNF mice were used in the SCI-CX3:BDNF group, and there were six mice in each group. In Additional Figure 1C, CX3:BDNF mice were used in the CX3:BDNF group, TMEM:BDNF mice were used in the TMEM:BDNF group, and there were six mice in each group. Angpt1: Angiopoietin-1; BDNF: brain-derived neurotrophic factor; PLX5622: colony-stimulating factor 1 receptor inhibitor; SCI: spinal cord injury; TUNEL: terminal deoxynucleotidyl transferase dUTP nick end labeling; VEGF: vascular endothelial growth factor.

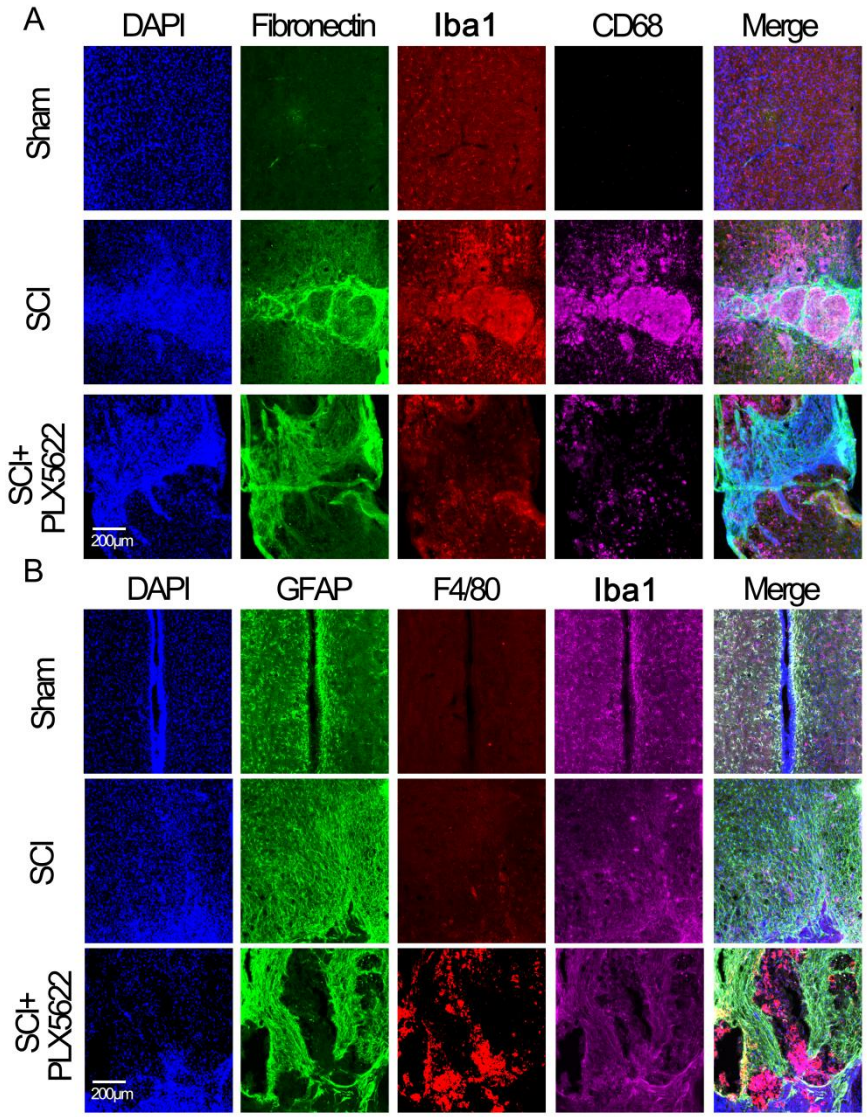

Additional Figure 4 Removal of microglia increases lesion size after spinal cord injury.

(A) High magnification of the center of the lesion shown in Figure 1E. Scale bar: 200 μm. Nuclei: blue, Fibronectin: green, Iba1: red, CD68: magenta. (B) High magnification of the lesion shown in Figure 1H. Scale bar: 200 μm. Nuclei: blue, Glial Fibrillary Acidic Protein (GFAP, marker of astrocyte): green, F4/80: red, Iba1: magenta. All groups of mice were WT mice, and there were six mice in each group. DAPI: 4',6-Diamidino-2-phenylindole; GFAP: glial fibrillary acidic protein; Iba1: ionized calcium binding adaptor molecule 1; PLX5622: colony stimulating factor 1 receptor (CSF1R) inhibitor; SCI: spinal cord injury.

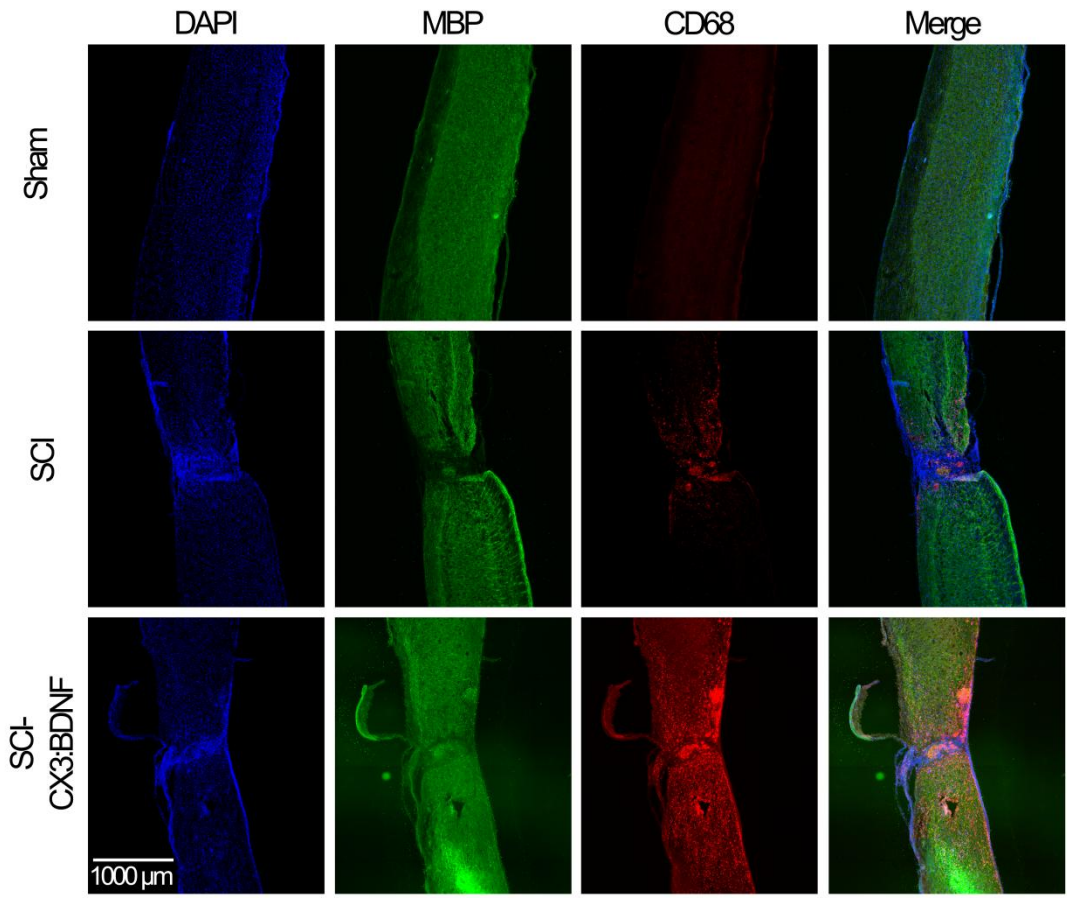

Additional Figure 5 BDNF overexpression by microglia resulted in sustained activation of microglia on day 28 after spinal cord injury.

Nuclei: blue, MBP: green, CD68: red. Scale bar: 1000 μm. C57BL/6J mice were used in the sham, SCI, and WT groups, CX3:BDNF mice were used in the SCI-CX3:BDNF group, and there were six mice in each group. BDNF: Brain-derived neurotrophic factor; DAPI: 4',6-diamidino-2-phenylindole; MBP: myelin basic protein; SCI: spinal cord injury.

Additional Table 1 Sequences of primers used for genotyping

Gene	Forward (5′ to 3′)	Reverse (5′ to 3′)
CX3CR1^{creER}-Mut	GTTAATGACCTGCAGCCAAG	ACGCCCAGACTAATGGTGAC
CX3CR1^{creER}-WT	AGCTCACGACTGCCTTCTTC	ACGCCCAGACTAATGGTGAC
BDNF-Mut	AGTCGCTCTGAGTTGTTATCAG	CACCTCGACCATGGTAATAGCG
BDNF-WT	AGTCGCTCTGAGTTGTTATCAG	TGAGCATGTCTTTAATCTACCTCGATG
TMEM119^{creER}-Mut	ATCGCATTCCTTGCAAAAGT	ACTTGGGGAGATGTTTCCTG
TMEM119^{creER}-WT	CAGTATGTGGGGTCACTGAAGA	ACTTGGGGAGATGTTTCCTG

BDNF: Brain-derived neurotrophic factor; Mut: mutant; WT: wild-type.

Additional Table 2 Sequences of primers used for quantitative reverse transcription-polymerase chain reaction

Gene	Forward (5′ to 3′)	Reverse (5′ to 3′)
BDNF	TGCAGGGGCATAGACAAAAGG	CTTATGAATCGCCAGCCAATTCTC
TGF-β1	GAGGCGGTGCTCGCTTTGTA	CGTTGTTGCGGTCCACCATTA
IL-1β	GACCTGTTCTTTGAAGTTGACG	CTCTTGTTGATGTGCTGCTG
TNF-α	AGACCCTCACACTCAGATCA	TCTTTGAGATCCATGCCGTTG
IL-10	GTCATCGATTTCTCCCCTGTG	ATGGCCTTGTAGACACCTTG
Bax	TGAAGACAGGGGCCTTTTTG	AATTCGCCGGAGACACTCG
Caspase-3	TGGTGATGAAGGGGTCATTTATG	TTCGGCTTTCCAGTCAGACTC
Bcl-2	GTGGTGGAGGAACTCTTCAG	GTTCCACAAAGGCATCCCAG
VEGFA	CTGCTGTAACGATGAAGCCCTG	GCTGTAGGAAGCTCATCTCTCC
GAPDH	AGGTCGGTGTGAACGGATTTG	TGTAGACCATGTAGTTGAGGTCA

TGF-β1: transforming growth factor β1; IL: interleukin; TNF-α: tumor necrosis factor-α; VEGF: vascular endothelial growth factor; GAPDH: Glyceraldehyde-3-phosphate dehydrogenase.